

การวิเคราะห์กระบวนการรีฟอร์มมิงเอทานอลสำหรับการผลิตไฮโดรเจน



นางสาว กิดาการ แสงเดือน

ศูนย์วิทยทรัพยากร

วิทยานิพนธ์นี้เป็นส่วนหนึ่งของการศึกษาตามหลักสูตรปริญญาวิทยาศาสตรมหาบัณฑิต
สาขาวิชาวิศวกรรมเคมี ภาควิชาวิศวกรรมเคมี

คณะวิศวกรรมศาสตร์ จุฬาลงกรณ์มหาวิทยาลัย

ปีการศึกษา 2551

ลิขสิทธิ์ของจุฬาลงกรณ์มหาวิทยาลัย

ANALYSIS OF ETHANOL REFORMING PROCESS FOR HYDROGEN
PRODUCTION



Miss Kidakarn Sangduan

ศูนย์วิทยทรัพยากร

A Thesis Submitted in Partial Fulfillment of the Requirements
for the Degree of Master Engineering Program in Chemical Engineering

Department of Chemical Engineering

Faculty of Engineering

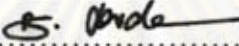
Chulalongkorn University

Academic Year 2008


Copyright of Chulalongkorn University

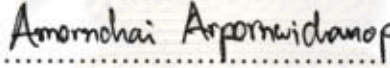
Thesis Title ANALYSIS OF ETHANOL REFORMING PROCESS FOR
HYDROGEN PRODUCTION
By Miss Kidakarn Sangduan
Field of Study Chemical Engineering
Advisor Assistant Professor Amornchai Arpornwichanop, D. Eng.

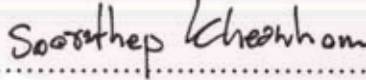
Accepted by the Faculty of Engineering, Chulalongkorn University in
Partial Fulfillment of the Requirements for the Master's Degree



..... Dean of the Faculty of Engineering
(Associate Professor Boonsom Lerdhirunwong, Dr.Ing.)

THESIS COMMITTEE


..... Chairman
(Associate Professor Tharathon Mongkhonsi, Ph.D.)


.....Advisor
(Assistant Professor Amornchai Arpornwichanop, D.Eng.)


..... Examiner
(Soorathep Kheawhom, Ph.D.)


..... External Examiner
(Woranee Paengjuntuek, D.Eng.)

ศูนย์วิจัยและพัฒนา
จุฬาลงกรณ์มหาวิทยาลัย

กิตติการ แสงเดือน : การวิเคราะห์กระบวนการรีฟอร์มมิงเอทานอลสำหรับการผลิตไฮโดรเจน. (ANALYSIS OF ETHANOL REFORMING PROCESS FOR HYDROGEN PRODUCTION) อ.ที่ปรึกษาวิทยานิพนธ์หลัก : ผศ.ดร. อมรชัย อภรณ์ วิชาฟ, 85 หน้า.

งานวิจัยนี้ศึกษาการวิเคราะห์ทางเทอร์โมไดนามิกของกระบวนการรีฟอร์มมิงด้วยไอน้ำ (steam reforming) และกระบวนการรีฟอร์มมิงแบบออโตเทอร์มัล (autothermal reforming) เพื่อการผลิตไฮโดรเจนจากเอทานอล โดยมีวัตถุประสงค์เพื่อหาสภาวะดำเนินงานที่เหมาะสมของระบบการผลิตไฮโดรเจน โดยคำนึงถึงเงื่อนไขของอุณหภูมิต่างๆที่ใช้ในการดำเนินงานและการเกิดโค้ก ผลการจำลองกระบวนการรีฟอร์มมิงด้วยไอน้ำและกระบวนการรีฟอร์มมิงแบบออโตเทอร์มัล แสดงให้เห็นว่าสารป้อนที่มีอัตราส่วนของน้ำต่อเอทานอลสูงจะช่วยเพิ่มการผลิตไฮโดรเจนและช่วยลดความเสี่ยงการสะสมของโค้กบนตัวเร่งปฏิกิริยา และมีการพบด้วยว่าในแต่ละอัตราส่วนของน้ำต่อเอทานอลจะมีอุณหภูมิดำเนินงานที่เหมาะสมสำหรับกระบวนการรีฟอร์มมิงด้วยไอน้ำเพื่อให้ได้ไฮโดรเจนปริมาณสูงสุด ส่วนการเกิดโค้กจะเกิดได้ดีที่อุณหภูมิในการดำเนินงานและอัตราส่วนของน้ำต่อเอทานอลต่ำ สำหรับกระบวนการรีฟอร์มมิงแบบออโตเทอร์มัลนั้น อุณหภูมิในการให้ความร้อนแก่สารป้อนเป็นตัวแปรที่ส่งผลกระทบต่ออัตราส่วนของออกซิเจนต่อเอทานอล อุณหภูมิในการให้ความร้อนแก่สารป้อนที่สูงสามารถลดปริมาณออกซิเจนที่ต้องการสำหรับการผลิตความร้อนแก่สารป้อนและปฏิกิริยาดูดความร้อนภายในเครื่องปฏิกรณ์ภายใต้สภาวะที่ระบบไม่มีการถ่ายเทความร้อนกับภายนอก กระบวนการกำจัดคาร์บอนไดออกไซด์โดยใช้เมทานอลเอทานอลามีน (MEA) เป็นสารละลายได้รับการศึกษาเพื่อลดการปล่อยก๊าซคาร์บอนไดออกไซด์และเป็นการทำให้ผลิตภัณฑ์ไฮโดรเจนมีความบริสุทธิ์ กระบวนการนี้สามารถทำให้ผลิตภัณฑ์ไฮโดรเจนที่ได้จากระบบรีฟอร์มมิงด้วยไอน้ำมีความบริสุทธิ์สูงถึง 97 เปอร์เซ็นต์โดยโมล

ศูนย์วิทยทรัพยากร

จุฬาลงกรณ์มหาวิทยาลัย

ภาควิชา.....วิศวกรรมเคมี.....ลายมือชื่อนิสิต.....กิตติการ แสงเดือน.....
สาขาวิชา.....วิศวกรรมเคมี.....ลายมือชื่อ อ.ที่ปรึกษาวิทยานิพนธ์หลัก.....อมรชัย อภรณ์.....
ปีการศึกษา.....2551.....

5070214921 : MAJOR CHEMICAL ENGINEERING

KEYWORDS : HYDROGEN / ETHANOL / REFORMING / ANALYSIS / SIMULATION

KIDAKARN SANGDUAN : ANALYSIS OF ETHANOL REFORMING PROCESS FOR HYDROGEN PRODUCTION. ADVISOR : ASST.PROF. AMORNCHAI ARPORNWICHANOP, D.Eng., 85 pp.

In this study, a thermodynamic analysis of steam reforming and autothermal reforming processes for the production of hydrogen from ethanol is performed. The aim is to determine optimal operating conditions for a hydrogen production system. Operational constraints, i.e., operating temperature and carbon formation, are taken into account. The simulation results on steam reforming and autothermal reforming show that feed stream with a high water-to-ethanol ratio is favorable for increasing hydrogen production and avoiding carbon deposition on catalyst. It is also found that at each water-to-ethanol ratio, there is an optimal temperature for steam reformer operation to provide the highest hydrogen yield. The carbon formation is favored at low operating temperatures and water-to-ethanol ratio. For autothermal reforming, a feed preheating temperature significantly affects oxygen-to-ethanol ratio; a higher preheating temperature can reduce the amount of oxygen required for preheating reactants and supplying endothermic reaction in the reformer under adiabatic condition. The carbon dioxide capture method using monoethanolamine (MEA) as solvent is studied in order to reduce carbon dioxide emission and purify hydrogen product. This process can purify hydrogen product stream from steam reforming system up to about 97 mol%.

Department :

Chemical Engineering

Field of Study :

Chemical Engineering

Academic Year :

2008

Student's Signature :

Kidakarn Sangduan

Advisor's Signature :

Amornchai Arpornwichanop

ACKNOWLEDGEMENTS

The author would like to express her deep sincere gratitude to her thesis advisor, Assistant Professor Amornchai Arpornwichanop, for his valuable suggestions, guidance and supervision throughout this thesis work. She would like to thank all teachers who have tendered for valuable knowledge to her at Chulalongkorn University

Moreover, she would like to express gratitude to all college members and friends at Department of Chemical Engineering, Faculty of Engineering, Chulalongkorn University for their warm support and helps over the entire period of this research.

Most of all, the author would like to express her highest gratitude to the member of her family for their moral support.



ศูนย์วิทยทรัพยากร
จุฬาลงกรณ์มหาวิทยาลัย

CONTENTS

	PAGE
ABSTRACT (Thai).....	iv
ABSTRACT (English).....	v
ACKNOWLEDGEMENTS.....	vi
CONTENTS.....	vii
LIST OF TABLES.....	x
LIST OF FIGURES.....	xi
NOMENCLATURES.....	xiv
CHAPTER	
I INTRODUCTION.....	1
1.1 Introduction.....	1
1.2 Objective.....	2
1.3 Scopes of work.....	2
II THEORY.....	4
2.1 Steam reforming reaction.....	4
2.2 Autothermal reforming reaction.....	5
2.3 Coke formation.....	6
2.3.1 The various parameters on coking process.....	8
2.4 Water gas shift reaction.....	9
2.5 Preferential oxidation reaction.....	10
2.6 CO ₂ capture method.....	11
2.6.1 Description of absorption process.....	13
2.6.2 Description of distillation.....	15

CHAPTER	PAGE
2.7 Thermodynamic equilibrium analysis.....	19
III LITERATURE REVIEWS.....	21
3.1 Hydrogen production technologies.....	21
3.2 Simulation studies of the reforming processes.....	27
3.3 Purification process for the production of hydrogen rich-gas....	30
3.4 Heat recovery of reforming systems.....	33
IV METHODOLOGY.....	37
4.1 Description of ethanol steam reforming process.....	37
4.2 Description of ethanol autothermal reforming process.....	40
4.3 Description of CO ₂ capture simulation using amine absorption.	42
V RESULTS AND DISCUSSION.....	45
5.1 Steam reforming.....	45
5.1.1 Effect of the water-to-ethanol molar ratio.....	45
5.1.2 Effect of reactor operating temperature.....	48
5.1.3 Analysis of steam reforming process.....	52
5.2 Autothermal reforming.....	53
5.2.1 Effect of the water-to-ethanol molar ratio.....	53
5.2.2 Effect of preheating temperature.....	55
5.2.3 Effect of oxygen-to-ethanol molar ratio.....	57
5.2.4 Analysis of autothermal reforming process.....	60
5.3 Comparison between steam reforming and autothermal reforming of ethanol.....	60
5.4 CO ₂ capture section.....	63

CHAPTER	PAGE
5.4.1 Effect of MEA concentration.....	63
5.4.2 Effect of circulation rate.....	64
5.4.3 Effect of number of stages.....	66
5.4.4 Effect of inlet gas temperature.....	69
VI CONCLUSIONS.....	72
REFERENCES.....	74
APPENDICES.....	78
APPENDIX A.....	79
APPENDIX B.....	81
APPENDIX C.....	82
VITA.....	85



ศูนย์วิทยทรัพยากร
จุฬาลงกรณ์มหาวิทยาลัย

LIST OF TABLES

		PAGE
Table 2.1	Feed factor on the relative coking rates under reforming condition of several pure hydrocarbons on alumina and used n-heptane as standard.....	8
Table 5.1	The optimal operating temperature of ethanol steam reforming at the different range of water-to-ethanol molar ratio	48
Table 5.2	The optimum conditions of ATR reaction for maximizing hydrogen production under adiabatic conditions.....	59
Table 5.3	Flow component of inlet gas and assumption for MEA concentration modeled case.....	63
Table 5.4	Flow component of inlet gas and assumption for CO ₂ capture circulation rate modeled case.....	65
Table 5.5	Flow component of inlet gas and assumption for absorber stages modeled case.....	66
Table 5.6	Flow component of inlet gas and assumption for absorber stages modeled case.....	68
Table 5.7	The assumption for absorber inlet gas temperature modeled case.....	70
Table B.1	Monoethanolamine property.....	81

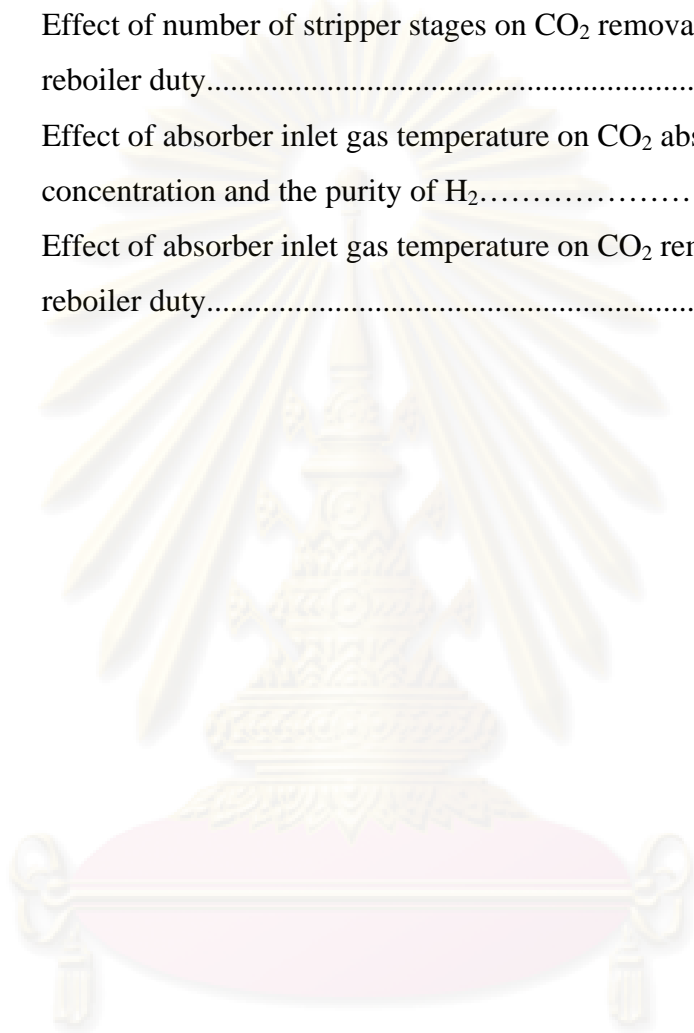
ศูนย์วิทยทรัพยากร
 จุฬาลงกรณ์มหาวิทยาลัย

LIST OF FIGURES

		PAGE
Figure 2.1	The steam reforming process with CO ₂ scrubbing.....	12
Figure 2.2	Absorber column.....	14
Figure 2.3	Distillation column.....	16
Figure 2.4	Stage flows.....	18
Figure 4.1	The steam reforming system components.....	37
Figure 4.2	The autothermal reforming system components.....	41
Figure 4.3	The CO ₂ scrubbing section components.....	43
Figure 5.1	Effect of R on carbon formation in SR reactor at 1 atm at each steam reforming temperature.....	46
Figure 5.2	Effect of R on the equilibrium compositions in SR reactor at 600 °C and 1 atm.....	47
Figure 5.3	Effect of stem reforming temperature on carbon formation in SR reactor at 1 atm.....	49
Figure 5.4	Effect of SR temperature on the equilibrium compositions at R = 2.0 and 1 atm.....	50
Figure 5.5	Effects of water-to-EtOH molar ratio and steam reforming temperature on hydrogen yields at 1 atm reactor pressure.....	51
Figure 5.6	The product compositions of reactor outlet stream in steam reforming process at R = 2.0, T _{SR} = 800 °C and P = 1 atm.....	52
Figure 5.7	Effect of water-to-ethanol molar ratio on carbon formation in ATR reactor at oxygen-to-ethanol molar ratio = 0.2 and pressure of 1 atm with varied preheating temperature in the range of 100 to 500 °C.....	53
Figure 5.8	Effect of water-to-ethanol ratio on the equilibrium compositions in ATR reactor at oxygen-to-ethanol molar ratio = 0.7, preheating temperature = 300 °C and 1 atm.....	54
Figure 5.9	Effect of preheating temperature on carbon formation in ATR reactor at R = 1.5 and 1 atm for each oxygen-to-ethanol molar ratio.....	55

Figure 5.10	Effect of preheating temperature on the equilibrium compositions in ATR reactor at oxygen-to-ethanol molar ratio = 0.7, R = 2.0 and 1 atm.....	56
Figure 5.11	Effect of oxygen-to-ethanol molar ratio on carbon formation in ATR reactor at R = 1.0 and 1 atm with preheating temperature in the range of 100 to 500 °C.....	57
Figure 5.12	Effect of oxygen-to-ethanol molar ratio on the equilibrium compositions in ATR reactor at $T_{\text{Preheat}} = 300$ °C, R = 2.0 and 1 atm.....	58
Figure 5.13	The product compositions of reactor outlet stream in autothermal reforming process at R = 2.0, $T_{\text{Preheat}} = 100$ °C and P = 1 atm.....	60
Figure 5.14	Comparison of equilibrium composition between steam reforming and autothermal reforming reaction at the preheating temperature = 100 °C and the optimal SR reactor temperature condition.....	61
Figure 5.15	Comparison of equilibrium composition between from steam reforming reaction at the optimal SR reactor temperature and autothermal reforming reaction at the same temperature of preheating and reactor.....	62
Figure 5.16	Effect of MEA concentration on CO ₂ absorbed concentration and the purity of H ₂	64
Figure 5.17	Effect of circulation rate on CO ₂ absorbed concentration and the purity of H ₂	65
Figure 5.18	Effect of circulation rate on CO ₂ removal and reboiler duty....	66
Figure 5.19	Effect of number of absorber stages on CO ₂ absorbed concentration and the purity of H ₂ product.....	67
Figure 5.20	Effect of number of absorber stages on CO ₂ removal and reboiler duty.....	67

	PAGE
Figure 5.21 Effect of number of stripper stages on CO ₂ absorbed concentration and the purity of H ₂	69
Figure 5.22 Effect of number of stripper stages on CO ₂ removal and reboiler duty.....	69
Figure 5.23 Effect of absorber inlet gas temperature on CO ₂ absorbed concentration and the purity of H ₂	70
Figure 5.24 Effect of absorber inlet gas temperature on CO ₂ removal and reboiler duty.....	71



ศูนย์วิทยทรัพยากร
จุฬาลงกรณ์มหาวิทยาลัย

NOMENCLATURES

SR	steam reforming
R	water-to-ethanol molar ratio
ATR	autothermal reforming
F_f	feed factor
HWGS	high water gas shift
LWGS	low water gas shift
WGS	water gas shift
PrOX	preferential oxidation
POX	partial oxidation
P	pressure
T_{SR}	steam reforming temperature
$T_{Preheat}$	preheating temperature
T_{ATR}	autothermal reforming temperature
R	ideal gas constant (8.314472 J/(mole K))
V_m	molar volume
ω	the acentric factor
T	absolute temperature
T_c	absolute temperature at the critical point
T_r	reduced temperature
p	absolute pressure
p_c	pressure at the critical point
Z	compressibility factor

CHAPTER I

INTRODUCTION

1.1 Introduction

Hydrogen is considered as one of the most promising energy carriers for the future. While fossil fuel is a finite supply of energy and emit green house gases into the environment, hydrogen is environmentally-friendly and clean energy source. Hydrogen can be efficiently converted into many useful energy forms. However, one of the major obstacles for a hydrogen energy system is the lack of hydrogen supplied in the energy carrier form. Generally, hydrogen can be produced from various sources (i.e., methane, methanol, ethanol, gasoline, etc.) using different technologies. The processes which are either currently implemented or under development include gasification, carbonization from coal, reforming process, electrolysis, and photocatalytic conversion (Seo et al., 2002). Among such technologies, the steam reforming (SR) process of hydrocarbon fuels is widely used for hydrogen production.

Considering various types of fuel for hydrogen production, the use of ethanol is interesting as it can be produced from renewable biomass sources. Ethanol can be converted to hydrogen at high thermal efficiency due to its high content of hydrogen atoms and low capital cost. Ethanol is effectively produced from a wide variety of biomass sources, including energy plant, sugar cane molasses, starch-rich materials, and agriculture residues via biochemical processes. In addition, the ethanol-to-hydrogen system has the significant advantage of being nearly CO₂ neutral. Along with the production process of hydrogen, CO₂ produced from reforming, water gas shift and preferential reactions can be consumed for biomass growth, offering a nearly closed carbon loop. The qualification of clean fuel is only true when the raw material is biomass. Thus, the use of ethanol for energy production is an effective solution for the reduction of CO₂ emissions (Perna, 2007).

It has been known that CO₂ is one of the leading greenhouse gases which has an severe effect on global warming crisis. Although the problem of CO₂ emission from hydrogen production could be relieved by biomass life cycle as mentioned previously, it takes a long time to reduce the amount of CO₂. To avoid the emission of CO₂ into the atmosphere, CO₂ must be concentrated, captured and sequestered.

Several techniques to remove CO₂ from flue gas have been studied and developed to reduce the cost of carbon capture. Among the alternatives for CO₂ recovery, the chemical absorption with amine aqueous solution is one of the most mature and less expensive technology (Mofarahi et al., 2008).

There are a number of reports concerning on an analysis of ethanol steam reforming (Francesconi et al., 2007; Ni et al., 2007). However, most previous studies have only focused on the performance evaluation of reformers, including a conventional fixed-bed reactor and a membrane reactor, with respect to key operating parameters (Giunta et al., 2008; Basile et al., 2008). In general, the system of steam reforming for hydrogen production consists of a steam reformer, a water gas shift reactor, and a preferential oxidation reactor.

In this work, the integrated systems based on ethanol steam reforming and autothermal reforming processes to produce hydrogen are presented. Thermodynamic analyses of two different types of the reforming system, which includes a reformer, a water gas shift reactor, and a preferential oxidation reactor, are performed with the aim to determine optimal operating conditions. A heat exchanger network is also considered in order to improve a heat integration process of available heat in the system. Furthermore, the CO₂ capture method is studied and applied to the ethanol reforming process for the production of hydrogen with high purity.

1.2 Objective

To analyze the effects of key operating parameters on the production of hydrogen from the reforming process of ethanol.

1.3 Scopes of work

In this study, an ethanol reforming process for hydrogen production is investigated. The ethanol reforming process consisting of a reformer, a water gas shift reactor, and a preferential oxidation reactor is simulated by using HYSYS simulator. The effects of various operating parameters, i.e., feed preheating temperature, reactor operating temperature, and water-to-ethanol molar feed ratio, on the production of hydrogen is presented. The heat integration of ethanol reforming processes is also considered. Furthermore, a chemical absorption process with amine aqueous solution for CO₂ capture is studied to separate CO₂ from hydrogen product stream. The CO₂ capture process comprises two columns: absorber and stripper column. In the former,

CO₂ is absorbed by amine aqueous solution where the used amine solution is recovered in the latter. The influences of key parameters, i.e., circulation rate, number of absorber and stripper stages, temperature of absorber inlet and reboiler duty, on the CO₂ removal and purity of hydrogen production are evaluated.



ศูนย์วิจัยทรัพยากร
จุฬาลงกรณ์มหาวิทยาลัย

CHAPTER II

THEORY

2.1 Steam reforming reaction

Steam reforming reaction is a high-temperature endothermic process, in which ethanol is converted into a gaseous mixture of H₂, CO, CO₂, CH₄ and unreacted EtOH and H₂O. The reaction is typically carried out at 550-800 °C that depends on the catalyst activity and the water-to-ethanol molar ratio (R) over NiO or Al₂O₃ catalysts. Because of an endothermic reaction, heat must be supplied to the system. The temperature of steam reforming reaction is limited at less than 800 °C in order to avoid the deactivation and thermal sintering of the catalyst and the deterioration of reformer.

The reaction pathways of the ethanol steam reforming are possible in many different routes due to the high operating temperature. Some of them are favored depending on the catalysts used (Benito et al., 2005). In practice, the following reaction schemes (Eqs. (2.1)-(2.4)) are usually employed to explain the steam reforming of ethanol:

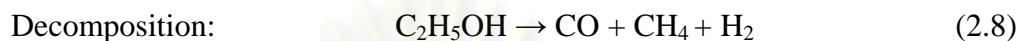
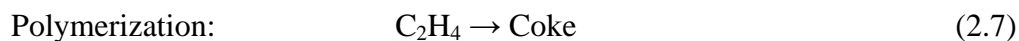
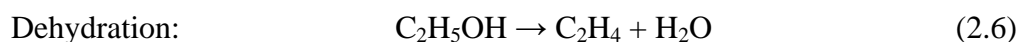


However, an ideal pathway for the ethanol steam reforming reaction with sufficient steam supply can be expressed in one-step conversion as shown in Eq. (2.5):



Furthermore, undesired pathway such as dehydration and decomposition that is source of coke formation since dehydration reaction produce intermediate products

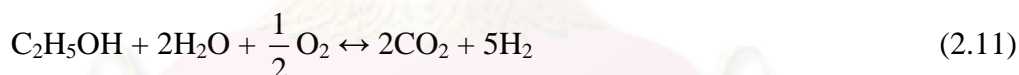
such as ethylene, which is easily transformed into carbon and low hydrogen production, can be occurred during reforming reaction progress.



In order to maximize hydrogen production, it is crucial to ensure sufficient supply of steam and to minimize ethanol dehydration and decomposition (Ni et al., 2007).

2.2 Autothermal reforming reaction

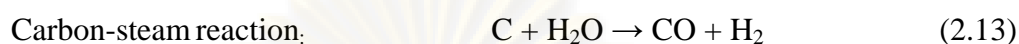
Autothermal reforming (ATR) is an exothermic reaction, which is a combination of ethanol oxidation and steam reforming reaction so the balance of the specific heat for each reaction becomes a very distinctive characteristic of this process. The total reaction of ethanol autothermal reforming can be written as



The ATR reaction can start quickly and continue without an additional/external heat supply. Moreover, the combination of these reactions can improve the reactor temperature control and reduce the formation of hot spots, avoiding catalyst deactivation by sintering or carbon deposition (Qi et al., 2005). The ATR process is capable of using heavy hydrocarbon as a fuel and the operating temperature of the process is in the range of 650-900 °C.

2.3 Coke formation

When reforming operating condition is a high-temperature step, reactants also undergo complex series of cracking reactions. These include methane decomposition and the reaction of carbon with steam.



Coke formation is occurred on the catalyst at the same time that ethanol is converted to H_2 and CO by decomposition reaction and it can be removed by reaction with steam as fast as it is formed.



Besides decomposition reaction, carbon can also be formed by boudouard reaction and CO reduction. These reactions are main source of carbon formation that is simultaneous carbon formation and gasification occurs.

Coke deposition that is a common deactivation mode in reforming process is formed and built up on the surface of catalyst, which results in hot spot in tubes. It can cause voids to form in the tube, increases pressure drop, reduces conversion of reactant and ultimately to ruptured tubes. Coke deposition is both of chemical and physical nature and occurs simultaneously under certain conditions when using hydrocarbon as a fuel. Coke deposition is a complex reaction, which results from the production of coke precursor and from their destruction, with multi-step reaction sequences and greatly differs by catalyst reactant system used. The formation of coke requires several metallic sites to block the metal and plug the support porosity lead to the catalyst deactivation by fouling.

Coke on the catalyst can be divided into two types: one is coke on metallic function and the other is coke on acidic support (Barbier,1987). In addition, Biwas et al. (1987) proposed coke on metal sites of the catalyst can be further distinguished into two types: reversible coke and irreversible coke. Reversible coke is easily removed by hydrogen, on the contrary, irreversible coke, which is graphitic coke, is more resistant to be removed by hydrogen. Coke formation is related to the acid-base

properties of the catalyst reactant system in which is investigated that strong acids rather than weak acids, Lewis acids rather than Bronsted acids favor coke formation (Tanabe et al., 1989). Metallic coke is produced early in the reforming reaction and is favored relative to acidic coke by operation under less severe condition due to acidic coke is more polymeric and is more difficult to gasify. Thus, there is only a small reaction between acidic coke and hydrogen is favored relative to metallic coke by operation under more severe conditions (Jaikeaw, 1995).

Since coke formation is always associated with main reaction by a cracking reaction either in the feed stream or in the various products, it is not possible to completely eliminate coke deposition. Although coke formation is inevitable, it can be slowed or prevented and some of its consequences can be avoid. The most popular method for reducing coke deposition is the addition of small amounts of alkali metal or metal such as tin, rhenium, which are call promoter, to reforming catalyst. This method results in the reduced acidity of the catalyst which decreases the cracking reaction that may occur. Moreover, this some additives can affect the selectivity, activity and lifetime of the catalyst. Indications exist that the use of rare earth oxides as supports can also reduce coking.

The deactivation of catalyst by coke deposit is an important problem which has long been of interest in reforming process. Coking on noble metal catalysts is well established that coke is deposited almost instantly as the reaction commences but deactivation as a result of coking takes many thousands of hours of operation. Virtually, the amount of coke deposited depends on carbon atoms in the feed and/or product stream due to molecules with large numbers of carbon atoms tends to produce coke deposits more easily. Gas phase reactions may lead to coke via free radical reactions which in turn may be influenced by the physical or chemical nature of the surface.

2.3.1 The various parameters on coking process

1) Feedstocks

The best feedstocks for steam reforming process are light, saturated, methane-rich streams and low in sulfur, i.e., natural gas or light refinery gas. When heavier hydrocarbons, including LPG and naphtha are used as feedstocks in hydrogen plant, the primary concern is coking of the reformer catalyst or in the preheater because the carbon is not removed fast enough by reacting of carbon with steam. The sort of feedstocks used affect to size of coking effect on the actual plant. Thus, a prereformer can be used in order to reduce risk of coking in system. It is an adiabatic catalytic fixed bed that is operated at a lower temperature. Gas leaving a prereformer is a gaseous mixture that contains only steam, hydrogen, carbon monoxide, carbon dioxide and methane. Furthermore, a prereformer can reduce the fuel consumption and steam production of reforming reaction.

Mieville (1991) introduced feed factor (F_f) which also affects coking rate and is suggested in Table 2.1.

Table 2.1 Feed factor on the relative coking rates under reforming condition of several pure hydrocarbons on alumina and used n-heptane as standard

Hydrocarbon	F_f
n-Heptane	1.0
Toluene	1.5
n-Nonane	2.0
Cyclohexane	7.0
2-Me-Pentane	7.5
Me-Cyclopentane	43
1-Hexane	90
Cyclohexane	540

2) Temperature

The addition of operating temperature can decrease coke deposition on the catalyst due to it reduces accessible metallic atoms of support (Lim, 1996).

3) Pressure

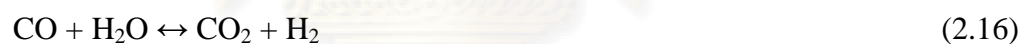
The steam reforming reaction is preferred to operate at low pressure. At this condition, it is found to affect coking process, which easily deposit on the catalyst. Moreover, lower pressure decreases coke formation on metal sites but increases coke formation on acidic support (Lim, 1996).

4) Water-to-hydrocarbon molar ratio

Coking may be partially alleviated by increasing the water-to-hydrocarbon molar ratio that can affect to the carbon-steam reaction. Control of coking by modification of water-to-hydrocarbon depends on the kinetics of the intermediate reactions.

2.4 Water gas shift reaction

Water gas shift reaction is the second important reaction in a reforming process. The reaction is an exothermic process, which brought CO in the syngas exiting from reformer down to lower level. CO is reacted, which is a fast reaction, with additional H₂O towards H₂ and CO₂. Thereby, leaving stream consist primarily of H₂ and CO₂. The CO conversion can be written as:



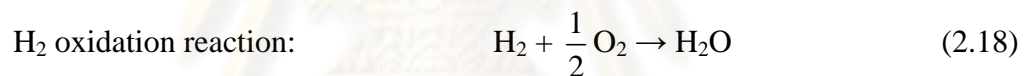
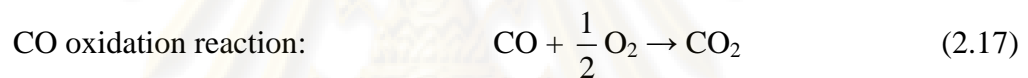
In contrast to reforming, shift conversion is favored by low temperature that its equilibrium constant decreases with temperature and the equilibrium is virtually insensitive to the pressure system. Shift reaction has two basic types that is high and low temperature. In general, operating temperature of high water gas shift (HWGS) reactor is in the range of 350 °C to 500 °C and employs a Fe/Cr catalyst. While low water gas shift (LWGS) reactor operates with a typical temperature of 150 °C to 250 °C in order to displace the equilibrium and use Cu/Zn/Al as a catalyst. The WGS reactor is expected to have the largest volume, and is limited by the catalyst intrinsic activity (Zalc et al., 2002).

As the shift reaction progresses, the heat reaction increases and the operating temperature limits the CO conversion, which is an incomplete conversion. Moreover, the operating temperature range must be limited for avoiding catalyst sintering at higher temperature and preventing water condensation and decreasing of reaction rate at lower temperature.

Due to the conversion achieved is limited by chemical equilibrium, water gas shift reaction rate is slower than the other reaction in reforming system. From this effect, WGS reactor will takes up the largest and heaviest unit in the fuel processor.

2.5. Preferential oxidation reaction

For using H₂-rich gas stream as an energy source of fuel cells, a small amount of CO, which is usually less than 1 %mole dry basis, after the water gas shift reaction is an unavoidable problem. Therefore, it is necessary to suppress CO to ppm levels for preventing irreversible damage on the fuel cell electrodes. The remaining CO would be removed by its conversion into CO₂ in a preferential oxidation (PrOX) process that is an exothermal step to producing a hot gaseous mixture in temperature range of 100-130 °C. Oxygen is used to proceed reaction with the following two oxidation reactions occur.



The H₂ oxidation is an undesirable reaction, which take place in order to combust some of H₂ content in synthesis gas. Because of this reaction is thermodynamically favored and H₂ concentration higher than CO concentration in the synthesis gas stream. Thus the suitable CO selective oxidation catalyst should be used to remove most of CO concentrations.

The many research of studies on CO selective have been published to evaluate various rate expressions for catalyst development. Noble metals such as Pt, Rh, Ru and Pd on alumina are commonly used for CO oxidation. These catalyst reactions are a highly exothermic, which increases reaction temperature.

The O₂ level is an important factor in PrOX process to improve the performance operation. In spite of theoretically only 0.5 mole of O₂ is needed to remove 1 mole of CO, most of PrOX reactors use excess air to some extent due to H₂ oxidation reaction (Choi et al., 2004). In order to generate a hydrogen rich gas stream that is applied to PEM fuel cells, it is important to remember that a small amount of

unconverted O_2 at PrOX stage will be able to produce microcombustion inside fuel cell anode and damage the polymeric membrane (Benito et al., 2007).

Besides two proposed oxidation reactions, equilibrium water gas shift reaction may be occurred in the temperature region at 200 °C with low concentration of H_2 and CO in gaseous mixture. At this condition, the forward reaction should be dominate, however, most PrOX reactor feed streams have large amounts of H_2 and CO, which are high enough to influence the reverse water gas shift reaction (Choi et al., 2004).

2.6 CO_2 capture method

Recently, there is a wide variety of separation method that is used to purify the synthesis gas since the gaseous mixture has a wide variety of components. The method selection depends on many factors, including investment and operating cost, end-use, and product purity required.

There are many processes for removal of CO_2 from gas mixture, which is generated from reforming and shift reactor, consisting of mainly H_2 , CO_2 and small amount of H_2O , CH_4 and CO. Chemical absorption is commercially technology that has been used successfully in the chemical, petroleum and gas industries for a long time to separate and recover CO_2 from synthesis gas. The steam reforming process with CO_2 scrubbing by using amine solution is showed in Fig. 2.1.

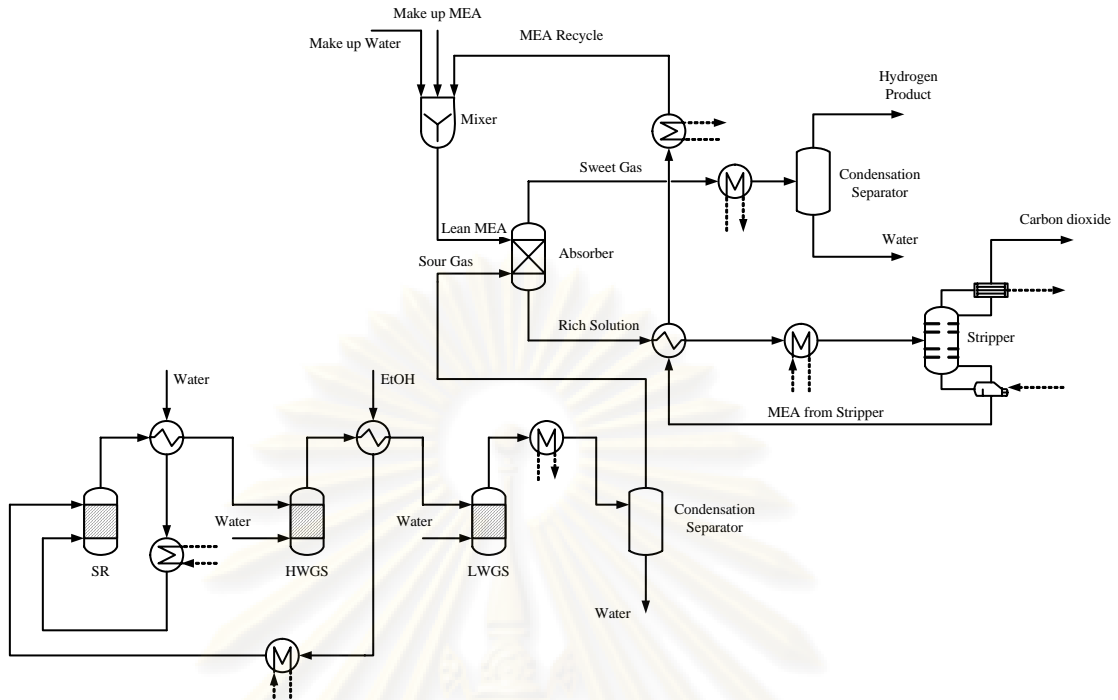
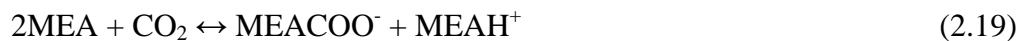


Fig. 2.1 The steam reforming process with CO₂ scrubbing.

This CO₂ capture method can operate when there is a low concentration (5-15 vol%) of CO₂ in a gaseous stream at atmospheric pressure. Chemical absorption process using amine aqueous solution consists of 2 separation steps:

1. After gaseous stream, including amount of CO₂ is fed to the absorber, amine solvent is added and absorbs CO₂ into the liquid solution at low temperature (40-65 °C). Selection of suitable solvent depends on acid-base neutralization reaction and it is applicable for low to moderate CO₂ partial pressure (3.5-21.0 kPa) i.e., diethanolamine (DEA), diglycolamine (DGA), methyldiethanolamine (MDEA) and monoethanolamine (MEA). In the absorber about 90% of the CO₂ contained in a gaseous stream can be formed a new compound in a reversible chemical reaction to a CO₂ solvent at a relatively low temperature and is separated out from the other gases.

CO₂ absorption by using amine solution has quite complex mechanisms. For this case study, aqueous solution of MEA is used as treating solvent. Therefore, CO₂ absorption reaction can be described by the following reaction:



$$\begin{aligned}
 P_{CO_2} &= \frac{K[MEA^+][MEACOO^-]}{[MEA]^2} \\
 &= K\alpha^2/(1-2\alpha)^2
 \end{aligned}
 \tag{2.20}$$

where $\alpha = CO_2 \text{ loading} = \frac{\text{Total } CO_2}{\text{Total MEA}}$

2. The rich CO_2 solution is sent to the stripper tower where the solvent is regenerated by raising temperature in the range of 100-150 °C and then the chemical bonds are decomposed thermally so that CO_2 come back out of solution. The CO_2 leaving stripper tower is cooled and can be diverted to storage. While, a lean solvent is sent back to the absorber in order to be reused at the beginning of scrubbing cycle starts again.

Although, the captured CO_2 has a high degree of purity, this capture process has a high consumption of thermal energy.

The absorption stripping system is particularly interesting because of its possibility to regenerate the solution continuously, thereby operating in an almost closed cycle (Mofarahi et al., 2008).

2.6.1 Description of absorption process

Absorption or gas absorption is a mass transfer unit operation used in chemical industry to separate gases by scrubbing a gas mixture with a suitable liquid called absorbent or to produce chemical product by feed inlet gas to react with raw liquid material. One or more of the component of the gas mixture dissolve, react or is absorbed in the liquid. The result of absorption is in forms a physical solution with the liquid or the new substance when chemical reaction is occurred in absorption process.

The object of gas absorption may be gas purification such as removal of air pollutants from process vented gases or contaminants from gases in production process, product recovery or production of solutions of gases for various purpose. One example for application of absorption processes is absorption of hydrochloric vapor by water in air pollution control application.

Gas absorption is usually operated in vertical column as shown in Fig. 2.2. Liquid or solvent is fed at the top of the absorber and the gas mixture flow into the bottom. The result of countercurrent flow of gas and liquid in absorber was in form solution or mixture of absorbed gas in liquid and left the absorber at the bottom.

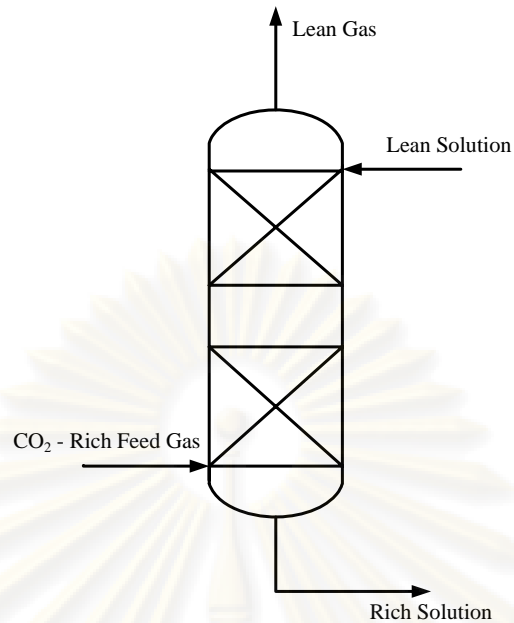


Fig. 2.2 Absorber column

Gas solubility

The solubility of the absorbed gas in liquid is considered with molecular diffusion in both gas and liquid phase to calculate the mass transfer rate.

At equilibrium condition, a component of a gas in contact with a liquid, gas phase is equal liquid phase fugacity. For ideal solutions Raoult's law can be used as relation

$$y_A = \frac{p_s}{P} x_A \quad (2.21)$$

where y_A is the mole fraction of A in the gas phase, P is the total pressure, p_s is the vapor pressure of pure A and x_A is the mole fraction of A in the liquid

For gas and liquid which condition nearly ideal solution molecules, Henry's law is applied in relation as:

$$y_A = \frac{H}{P} x_A \quad (2.22)$$

where H is Henry's constant and depend on temperature

A more general way to express solubilities of the vapor-liquid equilibrium by mean of constant m defined by

$$y = m x_A \quad (2.23)$$

the value of m also known as equilibrium K value

When Eqs. (2.21) or (2.22) is applicable at constant pressure and temperature equivalent to constant m in Eq. (2.23) a plot of y vs. x for a given solute is linear from the origin. Generally, for nonideal solutions or for nonisothermal conditions, y is not a linear function of x and must be determined from experimental data. The y - x plot, when used to absorber design, is called the equilibrium line (Reargmuang, 1997).

2.6.2 Description of distillation

The separation of liquid mixtures by distillation depends on differences in volatility between the components. The greater the relative volatilities, the easier the separation. The basic equipment required for continuous distillation is shown in Fig. 2.3. Vapor flows up the column and liquid counter-currently down the column. The vapor and liquid are brought into contact on plates, or packing. Part of the condensate from the condenser is returned to the top of the column to provide liquid flow above the feed point (reflux) and part of the liquid from the base of the column is vaporized in the reboiler and returned to provide the vapor flow.

ศูนย์วิทยทรัพยากร
จุฬาลงกรณ์มหาวิทยาลัย

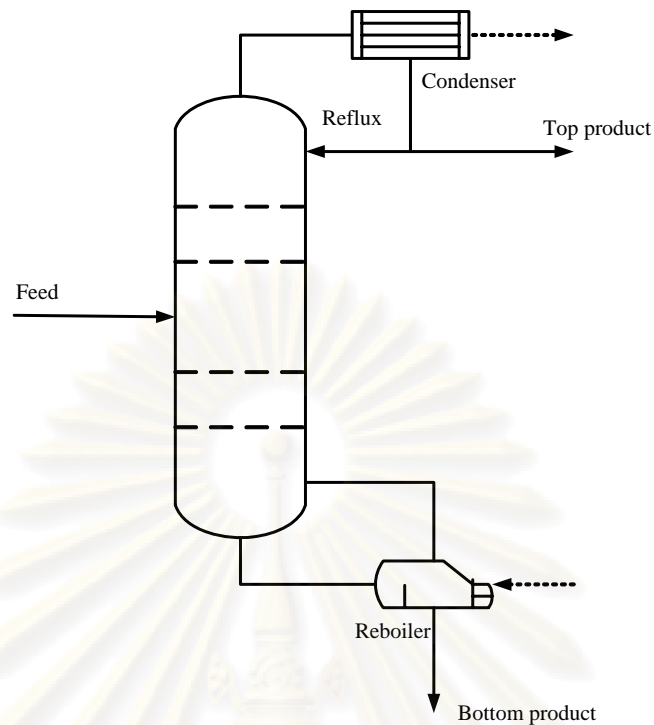


Fig.2.3 Distillation column

In the section below the feed, the more volatile components are stripped from the liquid and this is known as the stripper section. Above the feed, the concentration of the more volatile components is increased and this is called the enrichment or more commonly, the rectifying section. Fig.2.3 shows a column producing two product streams, referred to as tops and bottoms, from single feed.

If the process requirement is to strip a volatile component from a relatively non-volatile solvent, the rectifying section may be omitted and the column would then be called a stripping column.

In some operations, where the top product is required as a vapor, only sufficient liquid is condensed to provide the reflux flow to the column and the condenser is referred to as a partial condenser. When the liquid is totally condensed, the liquid returned to the column will have the same composition as the top product. In a partial condenser the reflux will be in equilibrium with the vapor leaving the condenser. Virtually pure top and bottom products can be obtained in a single column from a binary feed but where the feed contains more than two components, only a single pure product can be produced, either from the top or bottom of the column.

Several columns will be needed to separate a multi-component feed into its constituent parts.

Reflux considerations

The reflux ratio is normally defined as:

$$\text{Reflux ratio} = \frac{\text{flow returned as reflux}}{\text{flow of top product taken off}} \quad (2.24)$$

The number of stages required for a given separation will be dependent on the reflux ratio used.

In an operating column the effective reflux ratio will be increased by vapor condensed within the column due to heat leakage through the walls. With a well-lagged column the heat loss will be small and no allowance is normally made for this increased flow in design calculations. If a column is poorly insulated, changes in the internal reflux due to sudden changes in the external conditions, such as a sudden rain storm, can have a noticeable effect on the column operation and control.

Stage equation

Material and energy balance equation can be written for any stage in a multi-stage process.

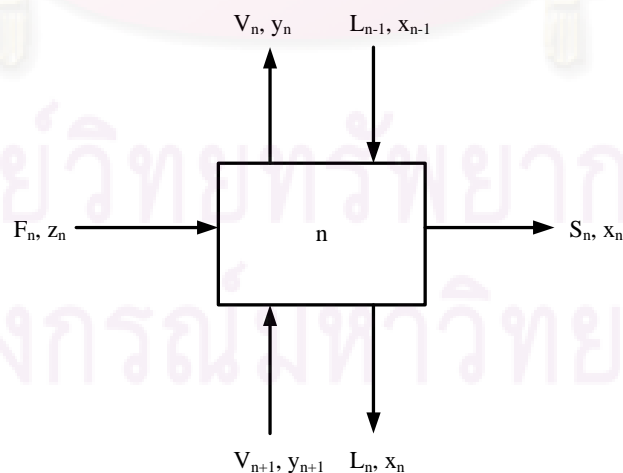


Fig.2.4 Stage flows

Fig.2.4 shows the material flows into and out of a typical stage n in a distillation column. The equations for this stage are set out below for any component i .

Material balance

$$V_{n+1}y_{n+1} + L_{n-1}x_{n-1} + F_n z_n = V_n y_n + L_n x_n + S_n x_n \quad (2.25)$$

Energy balance

$$V_{n+1}H_{n+1} + L_{n-1}h_{n-1} + Fh_f + q_n = V_n H_n + L_n h_n + S_n h_n \quad (2.26)$$

where V_n = vapor flow from the stage

V_{n+1} = vapor flow into the stage from the stage below

L_n = liquid flow from the stage

L_{n-1} = liquid flow into the stage from the stage above

F_n = any feed flow into the stage

S_n = any side stream from the stage

q_n = heat flow into, or removal from, the stage

n = any stage, numbered from the top of the column

z = mole fraction of component i in the feed stream (note, feed may be two-phase)

x = mole fraction of component i in the liquid streams

y = mole fraction of component i in the vapor streams

H = specific enthalpy vapor phase

h = specific enthalpy liquid phase

h_f = specific enthalpy feed (vapor+ liquid)

All flows are the total stream flows (moles/unit time) and the specific enthalpies are also for the total stream (J/mole).

It is convenient to carry out the analysis in terms of equilibrium stages. In an equilibrium stage (theoretical plate) the liquid and vapor streams leaving the stage are taken to be in equilibrium and their compositions are determined by the vapor-liquid equilibrium relationship for the system (see Eq. (2.23)) (Coulson et al., 1983).

2.7 Thermodynamic equilibrium analysis

A thermodynamic analysis of the process under an equilibrium condition can be performed by two traditional approaches:

1. Total Gibbs free energy of closed system at fixed temperature and pressure operating conditions must decrease when irreversible process is occurring and chemical equilibrium will be occurred when $(dG^t)_{T,P}$ equals to zero.

$$(dG^t)_{T,P} = 0 \quad (2.27)$$

This condition can be used to determine reaction components at equilibrium condition. This method is appropriate for a single reaction system and is called stoichiometric thermodynamic approach.

2. For any chemical equilibrium condition of closed system at constant temperature and pressure operation, total Gibbs free energy has a minimum value for all occurring conversion.

$$G^t = \sum_{i=1}^C n_i \bar{G}_i = \sum_{i=1}^C n_i \left(G_i^\circ + RT \ln \frac{\bar{f}_i}{f_i^\circ} \right) \quad (2.28)$$

The amount of component, n_i , which corresponds to the minimum in G^t , is constrained by conservation of atomic species. Thus the n_i must satisfy the following relation (Balzhiser,1972):

$$\sum_{i=1}^N a_{ji} n_i = b_j, \text{ for } 1 \leq j \leq M \quad (2.29)$$

The second method is called the direct minimization of Gibbs free energy or Non-stoichiometric thermodynamic approach, which has been favored for calculation of multiple reactions.

The several advantages of this method are as follows: (a) a selection of the possible set of reactions is not necessary, (b) no divergence occurs during the

computation, and (c) an accurate estimation of the initial equilibrium composition is not necessary (Adhikaria et al., 2007).

Although the both method are specified for closed system at fixed temperature and pressure, these can applied to opened system. Since equilibrium condition has been occurred, there is unchangeable condition, which always takes place when temperature and pressure are fixed.



ศูนย์วิทยทรัพยากร
จุฬาลงกรณ์มหาวิทยาลัย

CHAPTER III

LITERATURE REVIEWS

Hydrogen is widely considered as a clean energy intermediate for the future because of it has the highest energy content per unit of weight, compared with any other known fuel. Hydrogen can be efficiently produced from a wide variety of resources such as coal, biomass, natural gas and other hydrocarbons in large industrial reformer. It is regarded as a great potential energy carrier as a large quantity of hydrogen can be easily stored to be used in the future. As a consequence, a number of investigations focusing on simulation and optimization studies of hydrogen production processes have been reported and these will be discussed in this chapter.

3.1 Hydrogen production technologies

In general, technologies for the production of hydrogen are based on different processes (steam reforming (SR), partial oxidation (POX), autothermal reforming (ATR)). Each production technology has different of operating method, constraint, advantage, disadvantage and including a variety of costs and benefits with regard to the environment, economics, security and other concerns.

1. Steam reforming process is the most energy efficient commercialized technology currently available and is most cost-effective when applied to large, constant loads. Steam reforming will begin to take a very predominate role in the disposal of all of today's waste material. Attractive features of this technology including, ability to produce a consistent, high-quality synthesis gas product that can be used for energy production or as a building block for transportation fuels (methanol, ethanol, biodiesel, diesel and gas, etc.) and for other chemical manufacturing processes. Steam reforming allows operation at high pressure without expending work on air compression. Since the process has generated steam without the use of air or oxygen, the product gas is free of diluent nitrogen. Furthermore, the steam reforming reactor can utilize waste heat on the combustion side of the reactor.

The steam reforming technology has the disadvantage of slow start-up, which makes it more suitable for a stationary system rather than a mobile system. As steam reforming is an endothermic process, heat must be supplied to the system. Usually the

required heat for reforming is obtained by the combustion of a fuel in a burner. During the production of hydrogen, CO_2 is also produced. The steam reforming process in centralized plants emits more than twice the CO_2 than hydrogen produced. To avoid emission of CO_2 into the atmosphere, CO_2 can be concentrated, captured and sequestered. Sequestration in ocean is controversial because of possible adverse impact on the aquatic environment by the reduction of ocean water pH. Additional research and development is needed to identify more durable reforming catalysts; improve reforming efficiencies; develop advanced, separation and purification technologies; and reduce the cost of carbon capture and sequestration.

2. Partial oxidation process is an exothermic reaction that generates energy in the system since it does not require energy supply from external. Hydrocarbon feed with oxygen at high temperature, which methane production is minimal, to produce mixture gas. The advantages of this reaction are that it can use heavy oil as a fuel when heavy oil is available at low cost and generate hydrogen without a catalyst. Furthermore, this reaction has a quick response time and high reaction efficiency. There are drawbacks to partial oxidation for large-scale commercial process. Due to pure oxygen is then required by removing nitrogen, which acts mainly as a diluent, the capital cost for oxygen plant makes partial oxidation process high in capital cost. Partial oxidation exhibits lower overall efficiency since the heat of waste gas stream at the end of reaction cannot be reused, poorer fuel quality and requires a high operating temperature. Moreover, hydrogen selectivity of ethanol partial oxidation is generally low so this reaction is a less accepted commercial process to produce hydrogen.

3. Autothermal reforming is one of alternative reforming technology that presents a combination of steam reforming and partial oxidation in a single reactor. Autothermal reforming has received considerable attention for several advantages related to its relative compactness, lower capital cost and greater potential for economies of scale. Due to autothermal reforming is the least developed process, this process has limited commercial experience and is developing by numerous researchers. Since steam reforming creates more hydrogen than partial oxidation and partial oxidation consumes some hydrogen product, the overall hydrogen production is lower than steam reforming process.

The distinguished characteristics of three major technologies and their commercial uses were widely studied for the production of hydrogen from hydrocarbon feedstocks by numerous researchers in the past years.

Lwin et al. (2000) re-examine thermodynamic equilibrium of the steam reforming of methanol to cover the extended range of compounds suggested by literature to be involved in the reactions. The equilibrium concentrations are determined for different mixtures of these compounds at 1 atm and at different temperatures (360-573K) and at different steam/methanol molar feed ratios (0-1.5), by method of direct minimization of Gibbs free energy. The thermodynamic optimum condition for hydrogen production, when carbon and methane formations are not considered, occurs at 1 atm, 400K and a steam/methanol feed ratio of 1.5 with a hydrogen yield of 2.97 moles per mole of methanol. At feed ratios greater than 1.5, CO and DME concentrations can be further reduced, however, hydrogen yield cannot be raised above the theoretical limit of 3 moles per mole of methanol.

Seo et al. (2002) analyzed thermodynamically a favorable operating condition of hydrogen production from methane. The performance of three different types of reforming technology consisting of steam methane reforming (SMR), partial oxidation (POX) and autothermal reforming (ATR) were analyzed using AspenPlusTM simulator. The thermodynamic equilibrium in reforming reactors was calculated by using the method of minimizing the Gibbs free energy and the effects of operating parameters such as the preheat temperature of reactant feed, the composition and flow rate of air, methane, and water, and the operating pressure and temperature of reforming reactors were studied. It was found that the maximum allowable reactor temperature is less than 800 °C in order to avoid the deactivation of catalysts. Moreover, the favorable operating conditions avoiding the formation of coke were determined. They reported that each reforming reactor is expected to have its own favorable operating characteristics. The optimum steam-to-carbon ratio of the SMR reactor was 1.9 whereas the optimum air-to-carbon ratio of the POX reactor was 0.3 at a preheating temperature of 312 °C. For the ATR reactor, the optimum air-to-carbon ratio of 0.29 and steam-to-carbon ratio of 0.35 were observed at the preheating temperature of 400 °C.

Ersoz et al. (2003) considered the effect of operating parameters on the product distribution and conversion efficiency of an autothermal reactor fed by low and high molecular weight hydrocarbon mixtures (LHCM and HHCM). LHCM

consists of 33.6% hexane (C_6H_{14}), 28% hexane (C_6H_{12}), and 38.4% xyol (C_8H_{10}), which is similar to gasoline and the selected HHCM is $C_{12}H_{26}$. The autothermal reformer was operated under adiabatic and isothermal conditions. The results showed that increasing the ratio of oxygen to carbon decreases the generation of hydrogen and CO. The effect of steam-to-carbon ratio on hydrogen production is more pronounced at a lower oxygen and carbon ratio. CO formation is depressed at higher values of the steam-to-carbon ratio especially when the reformer is operated at higher temperatures.

Semelsberger et al. (2004) presented thermodynamic analyses of autothermal processes using five fuel; natural gas, methanol, ethanol, dimethyl ether and gasoline. The objective of this study is to identify optimum temperature ranges and probable product distributions for the process using the five fuels considered. The analyses calculate equilibrium product concentrations at temperature from 300 to 1000K, pressures from 1 to 5 atm and the water-to-fuel ratios are varied from 1 to 9 times the stoichiometric value. The optimal processing conditions are sought for the different fuels. The result shows that the maximum of natural gas optimizing objective function occurs at a temperature about 1000K and a water-fuel mole ratio of about 4. The optimal processing of methanol occurs at a temperature of about 400K and a water-fuel mole ratio of about 1.5. The maximum of ethanol optimizing objective function occurs at a temperature of about 540K and a water-fuel mole ratio of about 4 (a water-carbon mole ratio of about 2). The maximum of dimethyl ether optimizing objective function occurs at a temperature of about 420K and a water-fuel mole ratio of about 4 (a water-carbon mole ratio of about 2). The maximum of gasoline optimizing objective function occurs at a temperature of about 800K and a water-fuel mole ratio of about 9 (a water-carbon mole ratio of about 1.3). Moreover, the calculation also shows that the oxygen-containing substances (methanol, ethanol and dimethyl ether) require lower operating temperature than the non-oxygenated fuels (natural gas and gasoline). Using a simple optimum objective function shows that dimethyl ether has the greatest potential product content, followed by methanol, ethanol, gasoline and natural gas, respectively.

Francesconi et al. (2007) investigated a fuel processor based on a steam reforming process of ethanol to generate a hydrogen-rich gas. The steam reforming of alcohols involves a complex multiple reaction. In their study, two possible pathways are considered; the first analyzed route according to the mechanism proposed by Benito et al. (2005) for a Co/ZrO₂ catalyst and the second route is an ideal case where

no intermediate compounds are formed. For the reaction pathway case A, the maximum efficiency ($\eta_{\text{FCS}}^{\text{LHV}}$) of 38% occurs at $T_{\text{Ref}} = 709$ °C and water to ethanol molar ratio (R) = 4. The efficiency based on a higher heating value ($\eta_{\text{FCS}}^{\text{HHV}}$) is 35%. For the reaction pathway case B, the maximum efficiency in terms of $\eta_{\text{FCS}}^{\text{LHV}}$ and $\eta_{\text{FCS}}^{\text{HHV}}$ is 39% and 36%, respectively, at $T_{\text{Ref}} = 308$ °C and $R = 3.2$. The effect of water-to-ethanol ratio and reforming temperatures were also analyzed. The results showed that the hydrogen yield of the reformer increases with increasing the water-to-ethanol ratio and the reforming temperature.

Perna (2007) analyzed the ethanol steam reforming (SR) process with the aim at obtaining high hydrogen production. In the proposed process, the heat required for the SR reaction is obtained from the combustion of ethanol in a catalytic burner (CB). When a PEM fuel cell system is integrated with the SR based fuel processor, the operating conditions of the reformer is different from the case without the PEM system because the anodic off-gas recirculation that depends on the fuel utilization factor of PEM fuel cell reduces the amount of ethanol sent to the CB to supply the required heat. At a fixed molar ratio $\text{H}_2\text{O}/\text{EtOH}$, the ethanol molar flow rate that have to be processed in order to produce 1 mol of hydrogen decreases as the SR temperature rises and levels off at temperatures greater than 800 °C. The amount of ethanol required by the SR reactor decreases with increasing $\text{H}_2\text{O}/\text{EtOH}$ molar feed ratio, but for the ratio of higher than 3.0, a decrease in the ethanol requirement is less significant. The result showed that for the PEM fuel utilization factor of 0.85, the maximum efficiency (HHV) of the SR processor unit is 0.903 when it is operated at a molar feed ratio $\text{H}_2\text{O}/\text{EtOH}$ of 2.5, the reactor temperature of 700 °C, and preheating temperature of air and steam of 600 and 100 °C, respectively.

Benito et al. (2007) analyzed the integration of a hydrogen production process and a PEM fuel cell. A bioethanol steam reforming processor was designed to produce a CO-free hydrogen rich stream with the required quality that can supply to a PEM fuel cell. The hydrogen purification stages selected to reduce CO concentration are water gas shift and CO preferential oxidation. Energy and mass balances for several configurations were considered in order to optimize the processor efficiency and to design the different reaction stages. The process efficiency was closed to 74% to produce hydrogen rich stream. While a theoretical efficiency of a bioethanol processor coupled to a PEM fuel cell, which included a heat recovery system closed

to 30%. Moreover, a 1 kW processor was designed and built in order to analyze its performance in producing a CO-free hydrogen rich stream. A new catalyst, which is developed in the Institute of Catalysis and Petro-chemistry (ICP-CSIC), is selected for the steam reforming stage. This catalyst is tested more than 500 hr in continuous operation and more than 4000 hr for accumulated tests.

Vagia et al. (2008) investigate autothermal steam reforming of selected compounds of bio-oil using thermodynamic analysis. Equilibrium calculations employing Gibbs free energy minimization were performed for acetic acid, acetone and ethylene glycol in a broad range of temperature (400-1300K), steam to fuel ratio (1-9) and pressure (1-20 atm) values. The maximum hydrogen yield is achieved in equilibrium mixtures at 900K, similar to simple SR. The optimal steam to fuel ratio value for the acetic acid and the ethylene glycol is 6 and for acetone is 9. The effect of pressure decreases the hydrogen mole fraction at 20 atm about 23%, 24% and 27% for acetic acid, ethylene glycol and acetone, respectively. When the required oxygen enters the system at the reforming temperature, autothermal steam reforming results in hydrogen yield around 20% lower than the yield by steam reforming because part of the organic feed is consumed in the combustion reaction. The ratio of O_2 /fuel under optimum conditions [$T = 900K$, $S/F = 6$ (9 for acetone) and $P = 1$ atm] is 0.33, 0.26, 0.62 for acetic acid, ethylene glycol and acetone, respectively.

Li et al. (2008) study thermodynamic equilibrium of methane autothermal reforming by Gibbs free minimization for methane and H_2O or CO_2 conversions, H_2 yield and coke deposition as a function of H_2O -to- CH_4 ratio, CO_2 -to- CH_4 ratio, O_2 -to- CH_4 ratio, reforming temperature and pressure. The results showed that coke elimination should be done by increasing the reaction temperatures in CO_2 reforming while by increasing the steam fed in steam reforming. Moreover, the O_2/CH_4 ratios should be higher than 0.4 or H_2O/CH_4 ratios higher than 1.2 for oxidative steam reforming when the reaction temperature is higher than 700 °C. The optimal $CH_4/CO_2/O_2$ feed ratios 1:0.8-1.0:0.1-0.2 through the analysis of thermodynamic equilibrium in the oxidative CO_2 reforming were corresponding to the reaction temperature higher than 800 °C.

From several researches, steam reforming is demonstrated as the dominant method for producing hydrogen that also produces significant amounts of hydrogen. Steam reforming reaction takes place at high temperatures, making it requires high energy for reaction that can be obtained by the combustion of fuel gas or tail gas and

other heat sources. Autothermal reforming is an alternative technology to reduce required heat from external source. Moreover, it has been developed and applied to fuel cell in a small-scale.

3.2 Simulation studies of the reforming processes

A simulation study of a reforming process for hydrogen production is reported in several papers. The aim is to analyze the characteristics of each reaction, which involves in the system, and result of thermodynamic operating conditions. Mathematical model of the system is used to evaluate the efficiency and performance of fuel processors.

Seo et al. (2002) studied the thermal energy required in each of the reforming technology, which is already identified thermodynamically favorable operating condition, to generate a given amount of hydrogen from methane. Each system comprises a steam generator, heater, reforming reactor, heat exchanger and shift reactor, however, each system has a different configuration to the other. For example, the SR reforming system has a heat exchanger to supply the heat to the reforming reactor, while the POX and ATR system do not need any heat exchanger. The material and energy balances of all units in each reforming systems were evaluated to compare thermal energy required in term of energy cost. Simulations show that the CH_4 flow rates required to generate 1 mol s^{-1} of hydrogen are 0.385 mol s^{-1} for SR, 0.364 mol s^{-1} for POX and 0.367 mol s^{-1} for ATR when the heat-transfer efficiency was 0.8. The results showed that the POX reforming system has the lowest methane consumption rate. On the other hand, when the heat-transfer efficiency is lowered to 0.7, these values change to 0.364 mol s^{-1} for POX and 0.404 mol s^{-1} for the SMR. These evaluations reveal that the POX reforming system is superior to the other systems in terms of the energy cost to produce the same amount of hydrogen from CH_4 .

Lyubovsky and Walsh (2006) described a reforming processor for a fuel processing system converting methanol into hydrogen and mechanical work. The systems, which are modeled by using AspenPlusTM simulation software, consist of an ATR reformer operating at elevated pressures followed by a membrane based hydrogen separation, a membrane retentate burner and a turbine for mechanical power recovery. The high pressure membrane discharge stream is combusted and expanded through a turbine generating additional power. Only one heat exchanger is required in

the system to recover heat from the turbine exhaust stream. Methanol can be converted to CO and H₂ at much lower temperature that allows combining reforming and water gas shift steps with in a single reactor. Addition of steam to inlet mixture is preheated and vaporized by heat contained in the turbine exhaust stream. There are seven cases of system operation are studied in which system parameters and assumptions about the system performance. The systems modeling are represented in which base case with no WGS activity in the membrane unit and WGS activity is assumed in the Pd based membrane separator unit. This compact system for reforming methanol to hydrogen-rich gas stream can have overall reforming efficiency exceeding 89%. Overall fuel for electricity efficiency for the system is estimated to be about 48.5% when coupled with a PEM fuel cell and an electrical generator and limited mainly by the efficiency of the PEM fuel cell. The system operation is very sensitive to the operating pressure. When system pressure decreases from 15 to 5 atm, the efficiency decreases from 89 to 71% in spite of more stringent assumptions on the membrane performance at low pressure.

Lyubovsky and Walsh (2006) proposed a new high pressure approach to small-scale reforming system for converting methane into hydrogen-rich gas. The system is based on an autothermal reforming reactor followed by membrane-based hydrogen separation. The system co-generates pure hydrogen and mechanical power. Dry catalytic partial oxidation reactor (CPOX) is used to convert methane into synthesis gas and water is added between the CPOX and the WGS reactors and used to cool the stream. The membrane unit is used to separate pure hydrogen at ambient from the high pressure reformat mixture provided by the WGS reactor. The membrane is modeled as a two step process involving a flow split at constant system pressure in which a specified hydrogen content is segregated from the reformat stream followed by a pressure let-down that reduces the pressure of high purity hydrogen stream to atmospheric. The burner discharge stream is expanded from the system operating to atmospheric pressure through a gas turbine to produce mechanical work. The system can be viewed as a turbine cycle in which part of the heating value of the fuel is removed for alternative use prior to combusting fuel in the combustion chamber of the turbine. Total reforming system efficiencies approaching 80% were possible with electrical efficiencies about 40%. The system was expected to have small size, simplified control requirements and fast start up.

Giunta et al. (2007) described a process to produce hydrogen from ethanol steam reforming. The process system consists of ethanol steam reformer, water gas shift reactor and CO preferential oxidation reactor. Isothermal operation is assumed for the reforming reactor, which is the only reactor that consumes energy due to the endothermic characteristic of the reaction. While adiabatic operation for WGS and COPROX reactors is assumed. Ethanol/water feed ratio and ethanol steam reformer temperature, key variables of the system, are analyzed and their results are discussed. The efficiency in terms of the First Principle is about 57-64% and the efficiency in terms of a thermal engine cycle is about 47-56% for the fuel processor. All of the case analyzed, the efficiencies obtained are higher than internal combustion engines with the additional advantage that CO₂ concentration in the atmosphere is not increased. Despite this fact, it is possible obtain a sustainable system burning about 20-34% of the ethanol steam reformer effluent. That is, it is possible to develop a system in which the inputs are ethanol, water and air and the outputs are electricity, heat and basically CO₂ and water. The operational conditions of the WGS and COPROX are closer to the evolution of those corresponding to equilibrium, thus reducing the entropy of the system and increasing the availability of the energy to obtain useful work.

Francesconi et al. (2007) performed process simulations of a steam reforming for evaluating fuel cell system performance. The maximum efficiency of an ethanol process for hydrogen production was analyzed for PEM fuel cell. The fuel processor consists of steam reformer, high and low temperature shift reactors and preferential oxidation, which are coupled to a PEM fuel cell. The ethanol processor efficiency depended on the reforming operating condition. The results of different pathway show that the fuel processor efficiency of a complex multiple reaction system is $\eta_{FP}^{LHV} = 80.5\%$ and efficiency based on higher heating value is $\eta_{FP}^{HHV} = 80.6\%$. While, the processor efficiencies of an ideal case are $\eta_{FP}^{LHV} = 81.4\%$ and $\eta_{FP}^{HHV} = 80.6\%$. Total electric efficiency up to 35% based on the ethanol HHV was calculated. A net electric efficiency around 35% was calculated based on the ethanol HHV. The responsibilities for the remaining 65% are: dissipation as heat in the PEMFC cooling system (38%), energy in the flue gases (10%) and irreversibilities in compression and expansion of gases.

Huang and T-Raissi (2007) studied five processes combining separation and production of liquid hydrogen directly from methane and landfill gas. CH_4 autothermal is selected for production of H_2 from CH_4 in a Gibbs reactor operating isothermally. The energy required for CH_4 pyrolysis is derived from partial combustion of CH_4 . The intermediate generated from autothermal process undergo high and low temperature water gas shift reactions to produce more H_2 and CO_2 . Finally, gaseous mixture is separated by using cryogenic separation, which can be conceived in many flow diagrams, into individual components. H_2O and pure CO_2 are separated as liquids while the remaining gas mixture is distilled to separate the high purity gaseous hydrogen (GH_2) from CH_4 and CO and then at low temperature GH_2 is liquefied to liquid hydrogen (LH_2). A gaseous stream containing CH_4 and CO is not separated and is recycled to the recirculation. The total thermal efficiencies of the processes considered exceed 81% and 79% for methane and landfill gas, respectively. The highest energy efficiency calculated is 57% for methane and 51% for landfill gas with the assumption of 10% overall energy loss and 30% efficiency for the cryogenic process used. The ratio of CO_2 to H_2 mass in these processes falls between 3.027 g g^{-1} and 4.219 g g^{-1} . If the input electrical energy to the system is generated from a renewable resource, such as solar or wind, conversion of CH_4 to liquid H_2 via processes considered would be essentially zero emission.

Above several studied researches show that the simulation software and mathematical model are used to design hydrogen production process in order to investigate the effect of many factors to reforming system performance. Furthermore, the system is developed to have more efficiency and proven before applied to industries.

3.3 Purification process for the production of hydrogen-rich gas

A wide variety of reforming processes are used to purify hydrogen stream since the synthesis gas is available at a wide variety of compositions, flows and pressures. The impurities in the synthesis gas are CH_4 , CO , CO_2 and N_2 that are removed to any desired level. CH_4 , CO and CO_2 is the residual left after reforming reactor. N_2 , which is feed to reforming reactor with O_2 , is the most difficult to remove that requires additional adsorbent. N_2 extent results in a dilution effect that required a large reactor volume. Separation step modeling is selected and described below.

Alie et al. (2005) analyzed the CO₂ capture process, using a monoethanolamine (MEA) with a view towards minimizing the cost of implementation. A new method to simulate amine scrubbing using ASPEN Plus software, which also contributes to gaining more insight into the operation of process, is presented. The decomposition method is useful for simulating the entire integrated process flow sheet. This method is applied to three different CO₂ concentrations (molar fraction, wet basis): 3% (to simulate flue gas from a gas turbine), 14% (flue gas from a coal plant) and 25% (flue gas from a cement plant). The results from the decoupled flow sheet provided good initial estimates for the convergence of the integrated flow sheet. Furthermore, the results from the decoupled and integrated flow sheets are similar. As the number of trays in the absorber increases, the flow rate of lean MEA required decreases. As the lean loading into the absorber increases, the flow rate required for a given recovery increases. With a 12 stages absorber, for a given CO₂ concentration, the loading of the rich MEA stream is independent of the lean loading. The following factors lead to a decrease in reboiler duty of the stripper: increased loading of the lean MEA stream up to 0.30, an increase in temperature of the lean MEA stream at α (molar ratio of CO₂ to MEA in the lean MEA stream) \geq 0.25 and an increase in the number of trays. Because of the constraints with the number of trays at higher loading, a value of α of about 0.25 in this case results in a minimum Q_{reb} for all CO₂ concentrations studied.

Lyubovsky and Walsh (2006) designed the reformer system model using a membrane separation unit from which an essentially pure low pressure hydrogen stream is recovered. The membrane unit is used to separate pure hydrogen at ambient from the high pressure reformat mixture provided by the WGS reactor. The membrane is modeled as a two step process involving a flow split at constant system pressure in which a specified hydrogen content is segregated from the reformat stream followed by a pressure let-down that reduces the pressure of high purity hydrogen stream to atmospheric. Hydrogen flux across a membrane is highest at the inlet section, where the partial pressure approaches equilibrium, the flux decreases such that a significant increase in area of membrane is required to approach high separation coefficients. In the proposed process scheme, however, recovering the energy of hydrogen remaining in the membrane retentate by combustion and expansion through the turbine, relaxes the requirement for obtaining a very high level of hydrogen separation. As a result, membrane size can be reduced significantly.

Lyubovsky and Walsh (2006) modeled separator in the methanol reforming system simulation studied. The system shows the two different schematic. A membrane having WGS activity is modeled as a series of two membrane separators having an adiabatic equilibrium WGS reactor between them. While the model base case with no WGS activity in the membrane unit is modeled with WGS reactor followed by one membrane unit. The separator assumes that the membrane is catalytically inert and only removes hydrogen from the reformat stream. A membrane separator, which adds WGS activity, converts CO to additional H₂, thus increase H₂ partial pressure and separation through the membrane. However, model simulations showed that at 80% approach to thermodynamic equilibrium in both membrane segment ($\eta_1 = 0.8$; $\eta_2 = 0.8$) the heat remaining in the retentate stream was insufficient for vaporization of methanol and water at the ATR inlet and the model failed to converge. In order to achieve convergence of the model the membrane separation was decreased to 50 and 52% approach to equilibrium for the first and second membrane segments, respectively ($\eta_1 = 0.5$; $\eta_2 = 0.52$). The addition of WGS activity to the membrane may provide a significant size advantage to the system, however, by allowing the membrane to operate further from equilibrium separation where high hydrogen permeation rate could lead to reduced size and cost of membrane separation unit.

Huang and T-Raissi (2007) presented the cryogenic separation and purification process in order to utilize partial condensation to separate hydrogen from impurities with higher boiling points such as H₂O, CO, CO₂, CH₄ and hydrocarbons because of the high relative volatility of hydrogen as compared to these impurities. Cryogenic process can separate hydrogen from off-gas with very high recovery efficiency at higher purity levels than hydrogen stream obtained from PSA or membrane separation processes. A cryogenic process is used for both H₂ separation and liquefaction. This one-step process can substantially increase the efficiency and reduce costs because no PSA step is required. Furthermore, the integrated process results in no CO₂ emissions and minimal H₂ losses. In the cryogenic process, water vapor is separated in the first stage and liquid CO₂ is removed from the gaseous mixture in the second stage. In the final stage, H₂ is separated from the stream containing CO and CH₄ that are recycled into a steam reforming reactor to produce additional H₂ that is then mixed with the feed stream from an autothermal reactor. H₂

gas extracted is cooled at low temperature to form liquid H_2 , which high purity and without any H_2 losses. High purity liquid CO_2 is generated as a value add co-product that make it useful in a variety of applications. For an optimized flowsheet, the extent of H_2 recovery can be 99.99% with purity levels as high as 99.9999% and methane conversion efficiencies of up to 99.99%. As a by-product of liquid H_2 production, high purity liquid CO_2 is also generated as a value added co-product.

Mafarahi et al. (2008) investigated the design and simulation of CO_2 recovery from flue gases of Sarkhun gas refinery turbine. In the design of CO_2 recovery process, amine solvent i.e., diethanolamine (DEA), diglycolamine (DGA), methyldiethanolamine (MDEA) and monoethanolamine (MEA) are considered and the optimal absorber and stripper performance parameters for low energy consumption are estimated. The results show that DGA solvent is the best solvent with minimum energy requirement for recovery of CO_2 from flue gas at atmospheric pressure. Moreover, the solvent circulation rate is lower in comparison to the other solvents, which will also reduce operating and fixed cost. Results of simulation showed a recovery of CO_2 with 90 mol% for an absorber with 11 stages while DGA solution concentration is 62 wt% and DGA circulation rate is 340 kgmole/hr. Also the results show that at 2.4 MW for reboiler duty and 1 MW for condenser duty, the amount of CO_2 recovery is greater than 85 mol% for the stripper with 11 stages.

There are many factors, which are considered to select the best method of purification, include hydrogen recovery, investment and operating cost and product purity. Besides purification of hydrogen from synthesis gas, removal of CO_2 should be considered. Since emission of CO_2 produced from industries affects to change of the earth's climate.

3.4 Heat recovery of reforming systems

Due to the consumption of thermal energy is a key issue, heat integration of the reforming system has been evaluated. There are some papers that consider and give suggested the heat exchanger network as described below.

Francesconi et al. (2007) investigated the energy integration that had been used to determine the optimal operating conditions to be considered in the system. Maximum heat integration with in the system is necessary to achieve acceptable net electrical levels. The heat exchanger network was implemented using the LNG exchanger model that allowed analyzing the system energy integration by means of

the process integration method or pinch technology. The depleted fuel of the PEM fuel cell, which is formed by cathode and anode outlets, is burnt off in the post-combustion system. The generated heat is used to balance the energy requirement of the fuel processing section. When the energy content of the depleted fuel is not sufficient to satisfy the balance, some of ethanol is considered to fire in burner. After the exchange with the LNG unit, the exhaust gases are sent to expand in a turbine coupled to the air compressor. The net electric efficiency based on HHV is approximately 35%. The remaining 65% is accounted for: dissipation as heat in the PEMFC cooling system (38%), energy in the flue gases (10%) and irreversibility in compression and expansion of gases. The tasks that demand more energy are vaporizing and reheating of the reactive mixture (0.79 kW), the reformer reactor (0.41 kW) and the preheating of the exhaust gas to the burner (0.67 kW). Of the needed energy to drive the FCS auxiliaries, mainly pumps and blowers for water, ethanol, air and heat management, largest load is the air compressor (0.16 kW), which delivers air to the cathode compartments of the stack and to the PrOX reactor.

Huang and T-Raissi (2007) constructed five flowsheets for liquid H₂ production. These are determined heat recoveries in heat exchanger. The thermal heat energy generated in the process is recovered via many ideal heat exchangers so this process can be more efficient than the conventional liquid H₂ plants. There are five flowsheets of heat exchanger arrangement. The energy required for cryogenic separation of H₂ from a gas mixture consists of 2 parts: H₂ separation energy and H₂ liquefaction energy. The cooling energy input for separating components of a gas mixture can be recovered to a large extent by using heat exchangers.

Perna (2007) investigated the better operating conditions to optimize the efficiency of the PEM fuel cell system integrated with a steam reforming based fuel processor fed by ethanol as fuel. The overall efficiency of the PEM fuel cell system had been investigated as a function of the fuel utilization factor and the effects of the anodic off-gas recirculation had been evaluated. The heat required for the SR reaction was supplied to the SR reactor by a catalytic burner (CB) fed with the ethanol and, if the recirculation is provided, the anodic exhausts which depend on fuel utilization factor for PEM fuel cell. The preheating of ethanol is obtained by cooling the reformat gas to the PEM fuel cell stack temperature. The synthesis gas exiting from the SR reactor is cooled in heat exchanger before going to high water gas shift reactor by preheating the air feeding the CB. The fuel processor efficiency increases when the

fuel utilization factor decreases, because the anodic exhausts are sent to the CB of the SR reactor reduces the ethanol needed to produce the heat required by the SR reaction. Moreover, the results of the overall system efficiency for different fuel utilization factor show that the maximum efficiency is obtained for $T_{SR} = 700$ °C and $U_F = 0.85$ when the molar feed ratio $H_2O/EtOH$ are equal to 2.5. In order to obtain high reforming efficiencies, it is necessary that the thermal energy required to preheat the feed streams derives from an internal source, and not from the thermal integration is essential to achieve a high efficiency in the fuel processor unit and in the whole fuel cell power system. In the nominal condition of the PEM fuel cell system the overall efficiency is 0.43.

Giunta et al. (2007) described a process to produce hydrogen from ethanol steam reforming. The feasibility to carry out the energy integration was evaluated in order to improve the exploitation of the available heat. The process system consisted of ethanol steam reformer, water gas shift reactor and CO preferential oxidation reactor. The heat exchanger was carried out between two streams with temperatures which were not too different. This energy integration was demonstrated with efficiencies η_1 ranging 57-64% and η_2 ranging 47-56%. These efficiencies should be taken as a ceiling, since the working efficiency must include energy loss. At constant R, W_{net} increases with T_{REF} , and so does η_2 . However, $|\Delta H_{sys}|$ also increases, since a rise in T_{REF} has the effect of recovering heat from the burn exhaust gases. Thus, a drop in η_1 is observed. Moreover, the number of heat exchangers results in the overall efficiency because a large number of heat exchangers allow a better efficient heat recovery and also more electric power. Nevertheless, a higher system volume is required.

Benito et al. (2007) selected steam reforming process to study a thermodynamic analysis, since it can produce higher amounts of hydrogen from ethanol feed than other reforming process. Due to an external heat required of steam reforming, the steam reforming reaction heat is supplied by energy recovered from exothermic stages (water gas shift and preferential oxidation), exhaust gases not converted in the fuel cell operation and the ethanol combustion. To control the heat necessary to vaporize and subsequently overheat, PID electronic is used. Plate heat exchangers controlled by PID controller to adjust the temperature of the streams for

WGS and COPROX reactors, are placed before reaction stages. The efficiency closes to 28% at a steam/carbon ratio of 4.8 for a bioethanol processor-PEM fuel cell system, which includes a heat recovery system for off-gas from the fuel cell anode.

Many researchers attempt to improve overall efficiency of reforming system. In the heat integration method, heat exchanger is used to improve system efficiency. Hot stream is used to heat cold stream in order to reduce external heat demand. Some process, required heat supplies form burner that use feed or flue gas as a fuel.



ศูนย์วิจัยทรัพยากร
จุฬาลงกรณ์มหาวิทยาลัย

CHAPTER IV

METHODOLOGY

4.1 Description of ethanol steam reforming process

The energy integrated process model for hydrogen production, using ethanol as fuel is demonstrated. As this simulation case is developed for system design, the pressure drops, energy losses are neglected throughout the system. The operating pressure and ambient temperature are fixed at 1 atm and 25 °C respectively. The system is based on a steam reforming reactor, which is investigated by performing a thermodynamic equilibrium analysis for the products and reactants.

Fig 4.1 shows a flow diagram of the steam reforming system components considered in this case study. The process involves four stages including, ethanol steam reformer (SR), high and low temperature water gas shift reactor (HWGS, LWGS), preferential oxidation reactor (PrOX). System modeling is performed using HYSYS simulation software to develop the simulations and calculations of the fuel processing reactions.

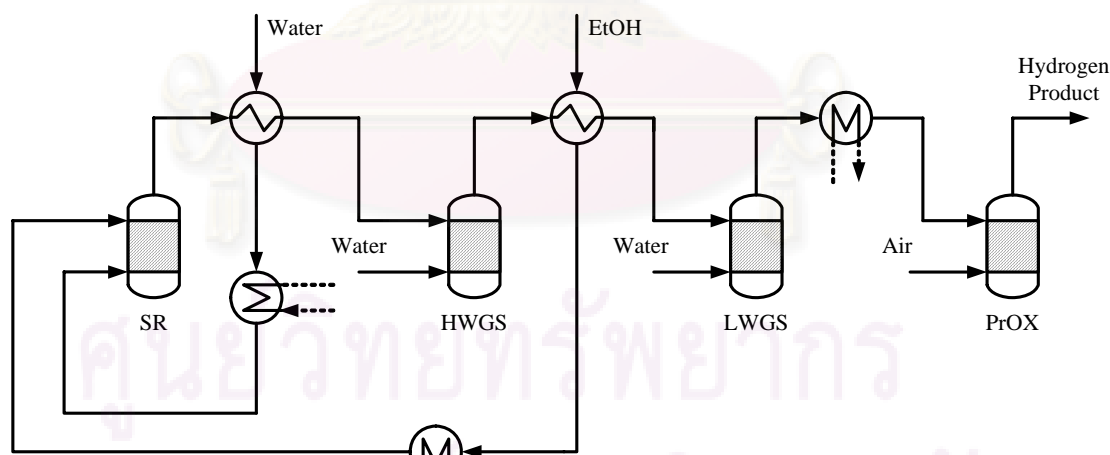


Fig. 4.1 The steam reforming system components.

4.1.1 Inlet streams

Ethanol and water are separately fed into the system at 25 °C and then two liquid feed streams are heated by heat exchangers. The proportion of water to ethanol, which entering the system, is controlled by water-to-EtOH molar ratio parameter (R) that can be written as follows:

$$\text{water-to-ethanol ratio (R)} = \frac{\text{Molar flow rate of steam}}{\text{Molar flow rate of EtOH}} \quad (4.1)$$

Kinetic studies claim that a high water-to-EtOH ratio in the feed improves the conversion in SR and WGS reactor but does not affect PrOX reactor performance (Giunta et al., 2007). The preheating of reactants is obtained by cooling the hot streams outlet from steam reforming reactor and HWGS reactor to adjust the temperature of the inlet streams. Fuels are fed to the reformer where the steam reforming reaction takes place, maintained at desired temperature. Preheated temperature of liquid fuels is not adjusted at temperature of less than 100 °C in order to heating the liquid reforming fuels to be a vapor phase. In this study, preheating temperature of each inlet stream before entering SR reactor is fixed at 100 °C. Since the significant amount of exchanged heat is consumed to evaporate water, supplied heat from external source is added when exchanged heat is not enough. Furthermore, the variation of the reformer preheating by exchanging inlet streams with hot stream results from the fixed operating temperature of reforming and HWGS unit.

4.1.2 Steam reforming reactor

In this simulation, SR reactor operates between 450 and 900 °C due to higher temperature can cause the catalyst deactivation by sintering. There are two main energy consumers in SR process such as preheating of fuel energy and supplying energy for endothermic reaction, which control the temperature of SR reactor. Inlet water, which corresponds to water-to-EtOH molar ratio, is varied from 0.5 to 10.0. The achievement of a product mixture is corresponding to thermodynamic equilibrium, which is based on minimizing the Gibbs free energy.

4.1.3 Water gas shift reactor

The leaving product stream and unconverted species from SR reactor pass through the WGS reactor where shift conversion takes place. The gaseous mixture inlet is supposed to be cooled down to the WGS reactor temperature and then combining stream with water before entering the reactor.

As the shift reaction progresses under adiabatic conditions, the heat reaction increases and the operating temperature limits the CO conversion, which is an incomplete conversion. The CO conversion is computed as

$$\text{CO conversion (\%)} = \frac{\text{Molar flow rate of reacted CO}}{\text{Molar flow rate of CO inlet}} \times 100 \quad (4.2)$$

The operating temperature range must be limited for avoiding catalyst sintering at higher temperature and preventing water condensation and decreasing of reaction rate at lower temperature. In this simulation, the operating temperature has been specified at 400 °C and 200 °C for the HWGS and LWGS reactor, respectively. These reactors are modeled as equilibrium reactors. An adiabatic operation has been considered for both WGS reactor, so input temperature variation modifies the output temperature.

4.1.4 Preferential oxidation reactor

Before entering PrOX unit, the LWGS reactor outlet is mixed with ambient air that is composed of 21% oxygen and 79% nitrogen in this studied system. PrOX reactor is operated at adiabatic condition, which using conversion reactor unit and the input temperature selected of the preferential oxidation reactor is 110 °C. O₂/CO ratio parameter is defined as the relationship between O₂ and CO flow rates that is written as follows:

$$\text{O}_2/\text{CO ratio} = \frac{\frac{1}{2} \times \text{Molar flow rate of O}_2}{\text{Molar flow rate of CO}} \quad (4.3)$$

In studied cases, O₂/CO ratio is taken as 1. This means that the amount of O₂ in added air is twice the CO concentration inlet. It oxidizes CO to CO₂ before the remaining O₂ totally oxidizes H₂ to H₂O that represents CO selectivity of about 0.33.

The selectivity of CO in PrOX reactor is defined as follows

$$\text{CO selectivity} = \frac{n_{CO}^{in} - n_{CO}^{out}}{(n_{H_2}^{in} - n_{H_2}^{out})} \quad (4.4)$$

CO and H₂ conversion are directly calculated from the concentration change of CO and H₂ by

$$\text{CO conversion (\%)} = \frac{\text{Molar flow rate of reacted CO}}{\text{Molar flow rate of CO inlet}} \times 100 \quad (4.5)$$

$$\text{H}_2 \text{ conversion (\%)} = \frac{\text{Molar flow rate of reacted H}_2}{\text{Molar flow rate of H}_2 \text{ inlet}} \times 100 \quad (4.6)$$

4.2 Description of ethanol autothermal reforming process

The hydrogen process model via autothermal reforming reaction, using ethanol as fuel for fuel cell is analyzed. The second simulation case is also developed for system design, the pressure drops, energy losses are neglected throughout the system. The operating pressure and ambient temperature are fixed at 1 atm and 25 °C respectively. The system is based on an autothermal reforming reactor, which is investigated by performing a thermodynamic equilibrium analysis for the products and reactants.

Fig 4.2 shows a flow diagram of the autothermal reforming system components considered in this case study. The process involves the same four stages as steam reforming system including, ethanol autothermal reformer (ATR), high and low temperature water gas shift reactor (HWGS, LWGS), preferential oxidation reactor (PrOX).

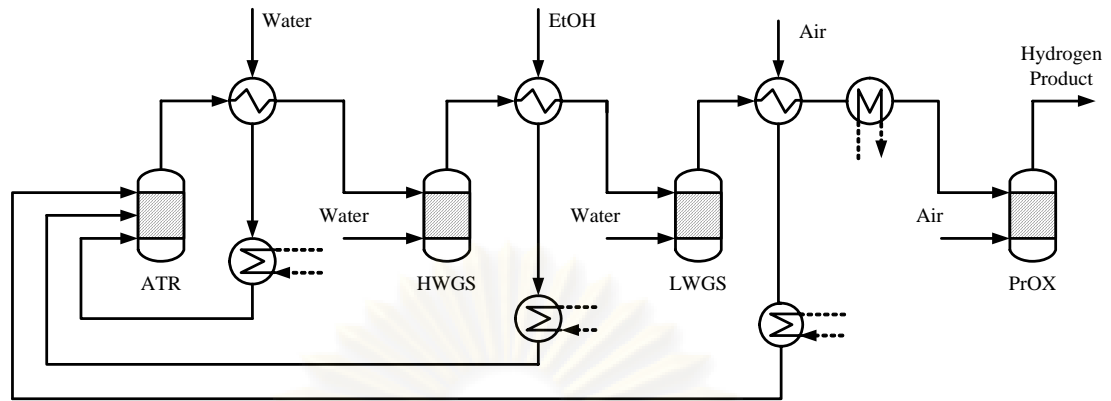


Fig. 4.2 The autothermal reforming system components.

4.2.1 Inlet streams

Ethanol, water and air are separately fed into the system at 25 °C and then three feed streams are heated by heat exchangers. Water is heated by the hot synthesis gas, which leaving from ATR reactor. HWGS leaving gas is used to heat ethanol inlet stream and LWGS leaving gas is used to heat air inlet that including 21 mol% of oxygen and 79 mol% of nitrogen. The proportion of water to ethanol, which entering the system, is controlled by water-to-EtOH molar ratio parameter (R) that is written in Eq. 4.1.

The proportion of oxygen to ethanol is controlled by oxygen-to-EtOH molar ratio parameter ($O_2/EtOH$), which can be written as

$$\text{Oxygen-to-ethanol ratio } (O_2/EtOH) = \frac{\text{Molar flow rate of oxygen}}{\text{Molar flow rate of EtOH}} \quad (4.7)$$

The gas feed streams are fed into the ATR reactor at the selected preheating temperature. The preheating temperature is varied in the range 100-500 °C, which corresponds to R ratio range of 0.5-10.0 and $O_2/EtOH$ ratio range of 0.1-1.0.

4.2.2 Autothermal reforming reactor

The ATR reactor is performed under adiabatic conditions that there is no heat transfer to or from reactor. The reactor temperature is calculated by adjusting input conditions i.e., oxygen-to-EtOH molar ratio, water-to-EtOH molar ratio and preheating temperature. Then thermodynamically favorable adiabatic operating

condition, which is based on minimizing the Gibbs free energy, in the ATR reactor is identified.

4.2.3 Water gas shift reactor

The leaving product stream from ATR reactor is cooled by exchanging with water inlet stream and then it is sent to HWGS reactor with some water at 400 °C. Before entering the LWGS reactor, gaseous mixture product is used to heat ethanol fuel. Then it is fed with water at 200 °C to LWGS reactor. These reactors are modeled as equilibrium reactors under adiabatic operation, so input temperature variation modifies the output temperature.

4.2.4 Preferential oxidation reactor

Before the synthesis gas is sent to PrOX reactor, the stream is exchanged heat with air to ATR reactor and then it is cooled again by using cooler. The synthesis gas is fed with a small amount of air to PrOX reactor at 110 °C in order to cleaning up the remaining CO. In this simulation, CO oxidation reaction is also selected at 0.33.

4.3 Description of CO₂ capture simulation using amine absorption

The CO₂ removal from synthesis gas process model at atmospheric pressure is shown in Fig 4.3. To demonstrate CO₂ absorption process, monoethanolamine (MEA) at a strength of 26 wt% in amine solvent is used as the absorbing medium. This process is considered the design parameters i.e., MEA concentration, solvent circulation rate, number of stages in absorber and stripper columns and temperature of absorber inlet gas.

This CO₂ removal process simulation uses the Amine Property Package and select Kent Eisenberg model to investigate the thermodynamic properties. The Kent Eisenberg model is limited to below 30 wt% MEA and below 120 °C since amine degrades at temperature above 120 °C.

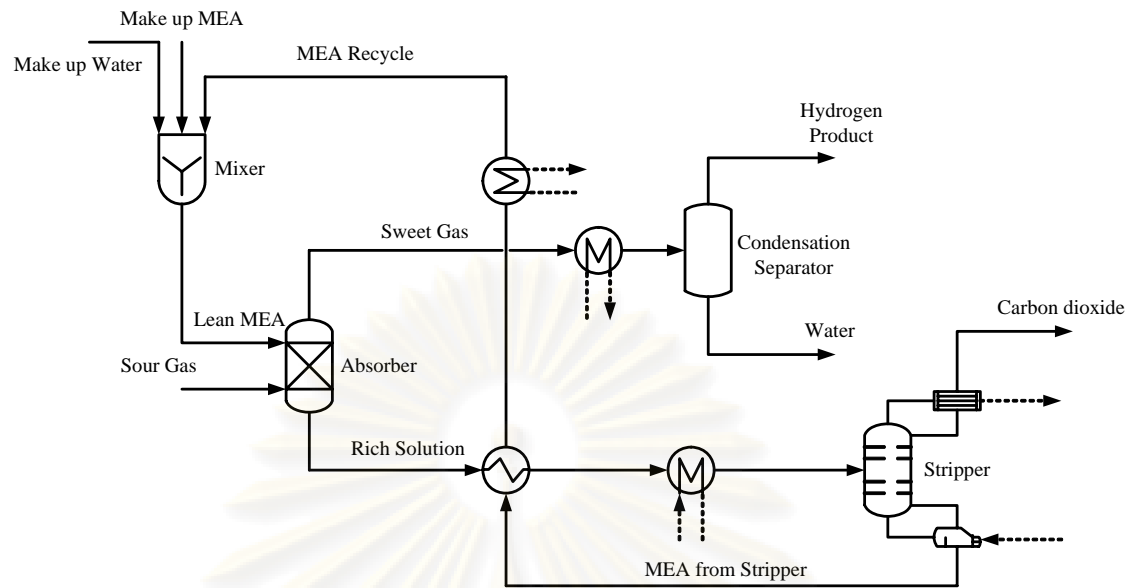


Fig. 4.3 CO₂ scrubbing section components.

4.3.1 Sour gas

First, the synthesis gas from hydrogen production system is cooled at a selected temperature in the range of 40-65 °C before entering a condensation separator in order to condense some water. Then gaseous mixture, which is described its thermodynamics by the Amines Property Package, is feed to the CO₂ absorber tower as a sour gas.

4.3.2 Absorber

Sour gas flows into the absorber at the bottom and lean MEA solution is fed at the top of the column. CO₂ gas is absorbed in the lean amine solution and then the rich solution is sent to stripper column in order to regenerate amine solution. While, the almost pure hydrogen gas as a top product is cooled to separate water and it is compressed to storage. Before entering the stripper tower, the CO₂-rich solution is heated by exchanging heat with regenerated MEA solution from stripper and it is heated again by heater to 100 °C.

4.3.3 Stripper

In the stripper tower, the solution is heated resulting in the release of CO₂ from the rich solution and then CO₂ product is cooled to condense water. The

regenerated MEA solution is cooled by using heat exchanger and cooler at designed temperature and then it is mixed with the make up water and MEA that are fed to keep the strength of MEA solution to be constant before sent back to the absorber section as lean MEA stream.



ศูนย์วิทยทรัพยากร
จุฬาลงกรณ์มหาวิทยาลัย

CHAPTER V

RESULTS AND DISCUSSION

5.1 Steam reforming

The effect of key parameters of steam reforming reaction i.e., water-to-ethanol molar ratio and reactor temperature on equilibrium compositions and coke formation is studied and discussed in this part.

5.1.1 Effect of the water-to-ethanol molar ratio (R)

The water-to-EtOH molar ratio (R) is found to affect significantly the formation of solid carbon, C(s) on the surface of catalyst. Carbon is generated at low R values with the operating temperature in the range of 500-900 °C at 1.0 bar reactor pressure. The results in Fig. 5.1 show that the formation of coke is strongly affected by the value of R more than the steam operating temperature. Deposition of coke can be removed by carbon-steam reaction as fast as it is formed. Though, the maximum value of R is restricted by cost of energy required of the steam reformer and the amount of hydrogen product. The simulation results of coke formation in the steam reformer can define the coking boundary, which should be avoided when the system is operated, is limited at R ratio below 2.8.

ศูนย์วิทยทรัพยากร
จุฬาลงกรณ์มหาวิทยาลัย

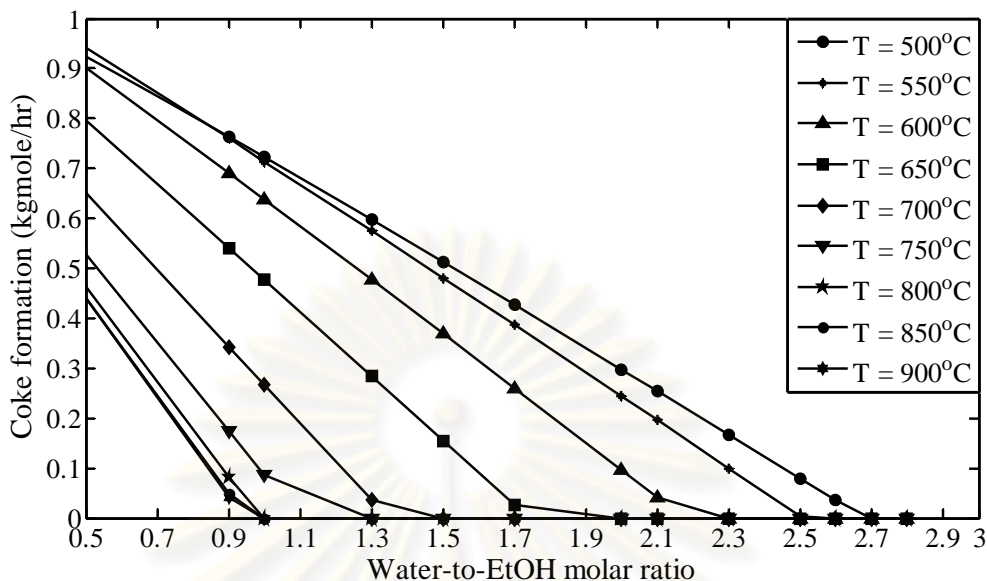


Fig. 5.1 Effect of R on carbon formation in SR reactor at 1 atm at each steam reforming temperature.

Influences of R that is varied from 0.5 to 10.0 for each operating temperature in SR reactor on equilibrium compositions are investigated at constant pressure of 1 atm. The results show that, at each operating temperature, there are same tendencies of each equilibrium composition. Fig. 5.2 shows result of R effect on the equilibrium compositions in SR reactor at 600 °C. To analyze the thermodynamic equilibrium of stream at the SR exit, many SR compositions that could be produced in SR reaction such as H₂, CO, CO₂, CH₄ and H₂O are found. A higher R is favorable for higher ethanol conversion and H₂ formation, which slightly increases until it is nearly constant. The CO₂ concentration also has a tendency as H₂ formation to be occurred, but its molar flow rate is lower than H₂ and is not greater than 2.0 kgmole/hr at each SR temperature. While the amount of H₂O increases steeply because of an unreacted H₂O by increasing R and H₂O generated from SR reaction. For the CO and CH₄ concentrations, the results have been divided into 2 groups based on the coking boundary. Both CO and CH₄ concentrations increase in the coking boundary, low value of R. Conversely, in the condition of no carbon formation, their concentration suppress in product stream by increasing R. At higher operating temperature, CH₄ concentration finally drops to zero.

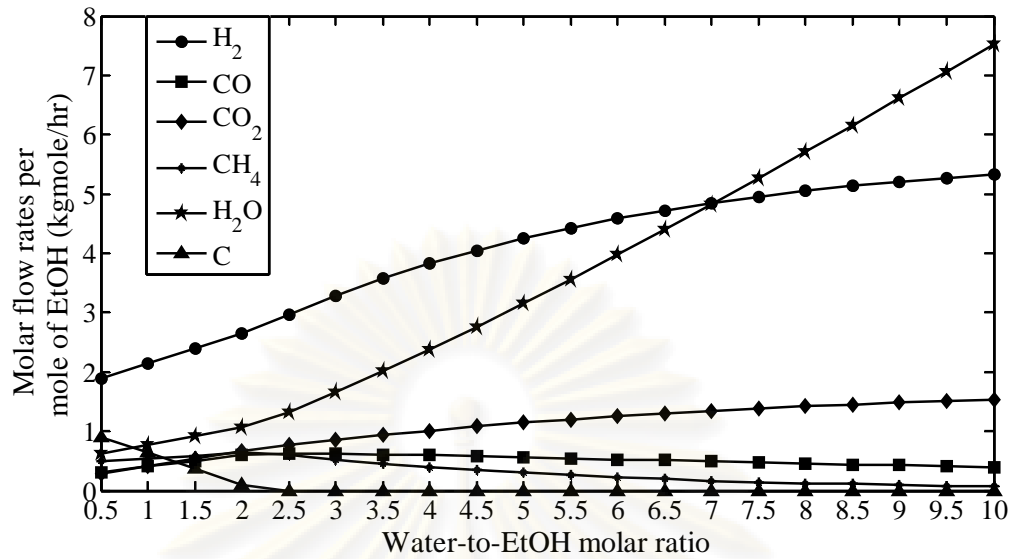


Fig. 5.2 Effect of R on the equilibrium compositions in SR reactor at 600 °C and 1 atm.

The high R value ensures a good behavior of reforming catalyst by avoiding carbon deposition on the active phase. Although, increasing R ratio neither increases ethanol conversion nor reduces CO formation significantly, a larger reactor size is required due to the larger gas volumes involved. Furthermore, it also increases reactor load and dilutes the product stream. In practice, the maximum of R is limited by the extra steam generation required that lead to the higher energy cost of the SR system. This some extra energy can be derived from the hot stream but it is not sufficiently for high R ratio to evaporate and preheating feedstock before entering to the SR reactor.

For each the R ratio range, there is an optimal temperature for reformer operation to provide the maximum H₂ yield and no coke formation. These data are listed in Table 5.1.

Table 5.1 The optimal operating temperature of ethanol steam reforming at the different range of water-to-ethanol molar ratio

Water-to-ethanol molar ratio ranges	Steam reforming temperature (°C)
1.0-3.1	800
3.2-4.7	750
4.8-7.7	700
7.8-13.2	650

For WGS reactors, effect of increasing R value result in CO conversion, which increases in both WGS reactors due to the WGS reaction is shift to H₂ formation with water excess. Moreover, if the R value is too low, the reducing environment is too strong and the catalyst can be reduced further that means amounts of hydrocarbons are formed over the high temperature shift catalyst. LWGS reaction can diminish CO with higher conversion than HWGS reaction, because of the equilibrium reaction is better at the lower temperature, thus the lower CO residual remain at the outlet stream.

The gaseous mixture from PrOX reactor is also obtained influence by rising R. Some amount of water is generated by combusting of some H₂, which is the other oxidation reaction that takes place in this reactor. The outlet temperature is decreased in accordance with high water excess. At lower R, CO concentration that is increased in SR reactor result in high CO value in PrOX inlet stream. Some H₂ are consumed with oxidation reaction in order that reduce CO to lower level required. This effect reduces H₂ yield at product stream. But then CO inlet is diminished, loss of H₂ product also lower by consuming a small amount of H₂ in oxidation reaction.

5.1.2 Effect of reactor operating temperature

The steam reforming temperature also is one of the critical influences to carbon build-up that gives the results in Fig. 5.3. At a fixed pressure, coke increases to a peak and then reduces to zero with R ratio of 1.0 and more by raising operating temperature. Although, increasing the operating temperature diminishes carbon formation, only increasing the operating temperature at R less than 1.0 cannot completely suppress solid carbon. Moreover, the operating temperature is limited at

800 °C that is the maximum operating temperature. Thus the value of R should be maintained at 1.0 or more in order to avoid coke formation. These results show that the formation of coke is strongly affected by the value of R more than the steam operating temperature.

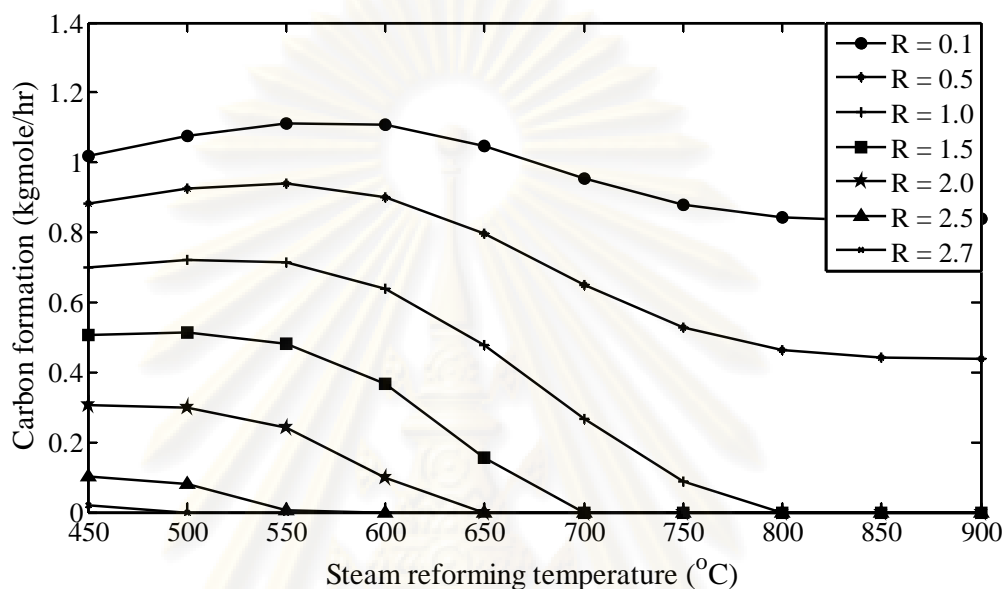


Fig. 5.3 Effect of stem reforming temperature on carbon formation in SR reactor at 1 atm.

The reforming temperature is studied at 450-900 °C to analyses concentration of equilibrium compositions and heat required. In practice, the steam reforming reactor can operate at 550-800 °C; higher temperatures cause the deactivation of the catalyst by sintering and the damage of the reactor. As the reactor operating temperature is fixed at a constant value, the preheating temperature of the reactants does not affect the equilibrium compositions in the steam reformer. On the other hand, the preheat temperature affects the heat duty that can reduce the heat supplied to the steam reformer. At a fixed R, the amount of hydrogen generated from 1 mole of ethanol increases steeply as the steam reforming temperature rises until it reaches the highest H₂ production of each R ratio then yield decrease gradually with increasing temperature. High reforming temperature is results in the higher thermal energy required to operate the endothermic reaction, which demands heat from external source. All results of varied operating temperature in SR reactor with each R ratio on

equilibrium compositions show the same tendency. Fig. 5.4 shows the variation of the SR products with constant R of 2.0 in operating temperature range (450-900 °C) and pressure is fixed at 1 atm. To analyze equilibrium compositions of the SR reactor, the amount of H₂ has a tendency to be rapidly increased with rising temperature at first. With the lower R ratio range, in spite of maximum H₂ production is derived from SR reaction at high operating temperature, the optimal operating temperature with the higher R ratio range decreases. A gradual decline in the amount of CH₄ is occurred with increasing SR temperature and finally drops to zero, while CO concentration sharply increases at first and then moderately rise for each constant R. Besides, SR temperature increased is the result of sharply diminishing H₂O to the minimum concentration when H₂ concentration increase at first and then the amount of H₂O is slowly increased later. The tendency of CO₂ is conversely to H₂O; CO₂ concentration raises to the maximum at about 550-600 °C and it reduce after.

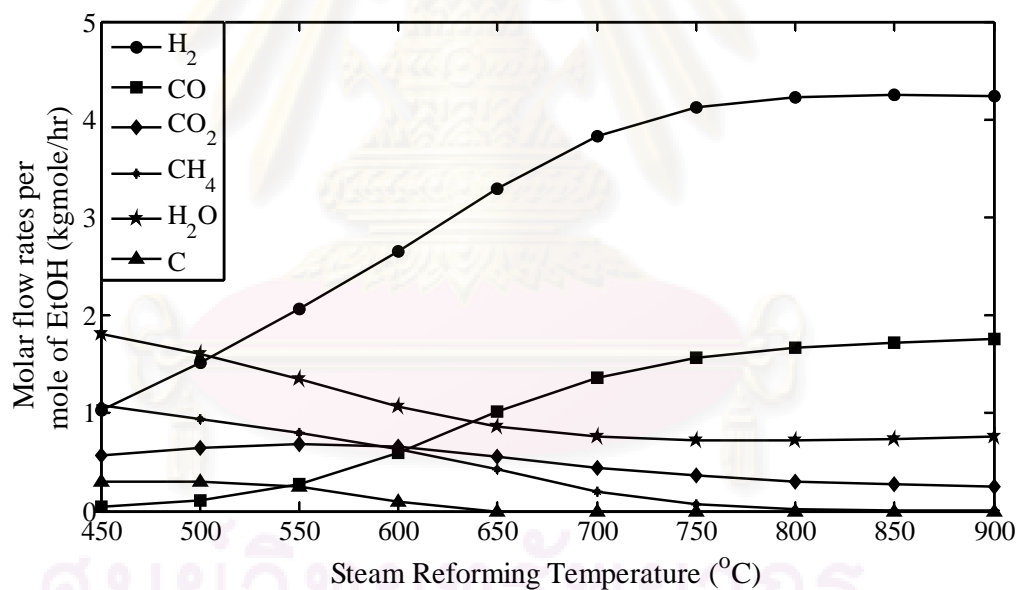


Fig. 5.4 Effect of SR temperature on the equilibrium compositions at R = 2.0 and 1 atm.

Results of water-to-ethanol molar ratio (R) and steam reforming temperature to H_2 concentration at 1 atm are summarized in a 3D surface, Fig. 5.5.

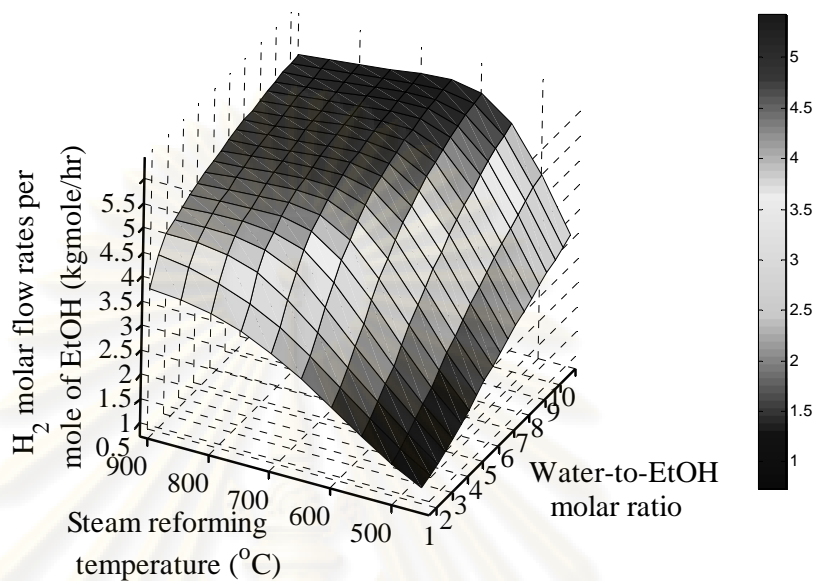


Fig. 5.5 Effects of water-to-EtOH molar ratio and steam reforming temperature on hydrogen yields at 1 atm reactor pressure.

ศูนย์วิทยทรัพยากร
จุฬาลงกรณ์มหาวิทยาลัย

5.1.3. Analysis of steam reforming process

Fig. 5.6 shows the output process stream compositions of main process units obtained at its operating conditions. After leaving the reformer, additional H_2 is obtained by shift reaction and then a small amount of H_2 is consumed in PrOX reactor. The decrease of mole fraction of H_2 after leaving each reactor is the dilution effect of both additional H_2O and nitrogen. While CO is continuously reduced in the cleaning method including water gas shift and preferential oxidation reaction to low level.

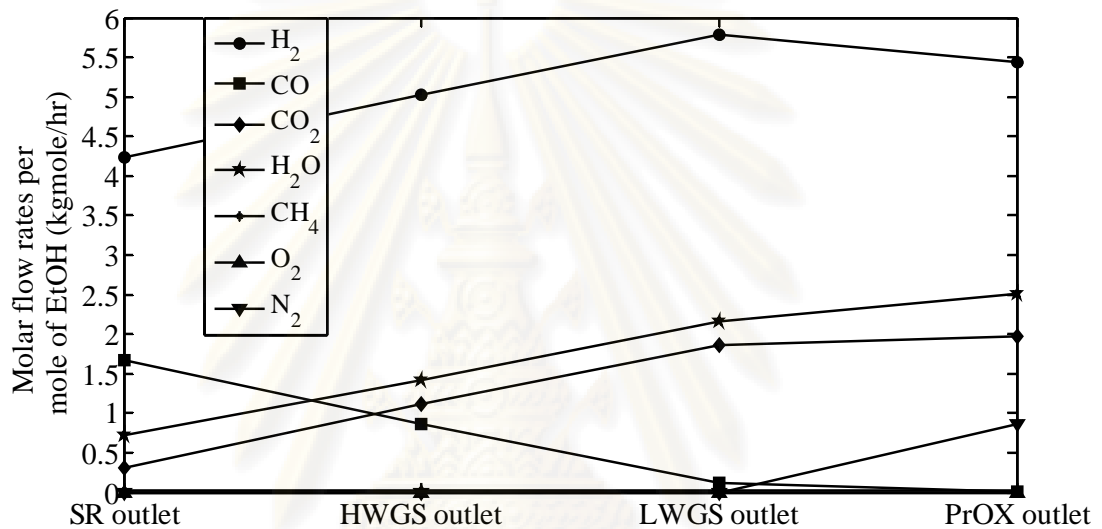


Fig. 5.6 The equilibrium compositions profile for steam reforming process at $R = 2.0$,
 $T_{SR} = 800\text{ }^{\circ}\text{C}$ and $P = 1\text{ atm}$.

ศูนย์วิทยทรัพยากร
 จุฬาลงกรณ์มหาวิทยาลัย

5.2 Autothermal reforming

The effect of key parameters of autothermal reforming reaction i.e., water-to-ethanol molar ratio, preheating temperature and oxygen-to-ethanol molar ratio on equilibrium compositions and coke formation is studied and discussed in this part.

5.2.1 Effect of the water-to-ethanol molar ratio (R)

The water-to-EtOH molar ratio (R) is also significantly affects the carbon formation that is generated at low value of R.

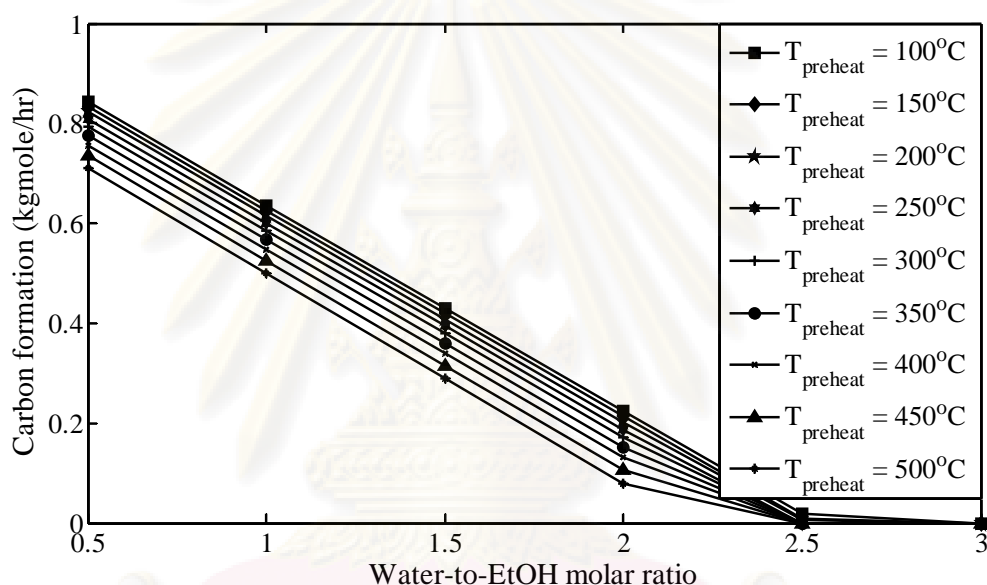


Fig. 5.7 Effect of water-to-ethanol molar ratio on carbon formation in ATR reactor at oxygen-to-ethanol molar ratio = 0.2 and pressure of 1 atm with varied preheating temperature in the range of 100 to 500 °C.

The effect of varied water-to-EtOH molar ratio on carbon formation is presented in Fig. 5.7. This result shows that the increase of R rapidly reduces the deposition of carbon at a constant preheating temperature. Furthermore, at R higher than 2.6, carbon is not generated in the reactor.

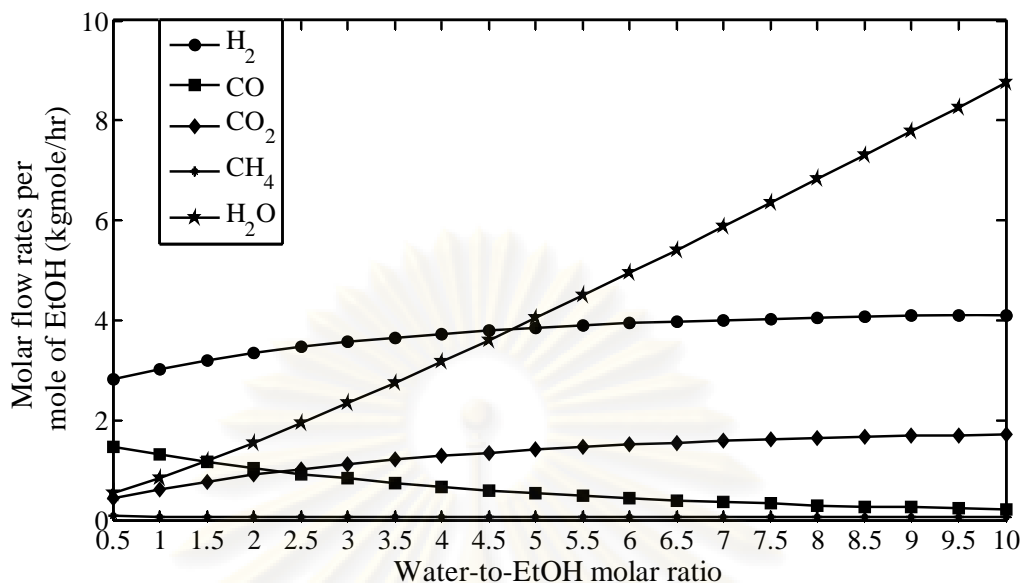


Fig. 5.8 Effect of water-to-ethanol ratio on the equilibrium compositions in ATR reactor at oxygen-to-ethanol molar ratio = 0.7, preheating temperature = 300 °C and 1 atm.

The result of R, which is varied from 0.5 to 10.0, on the conversion of components in Fig. 5.8 shows that H₂ and CO₂ are slightly generated with increasing R until it is nearly constant in the higher range of R. While, the amount of H₂O more steeply increases since there are more unreacted H₂O than SR reaction and generated H₂O from ATR reaction. The effect of remaining H₂O in ATR increases the size of the system units. It should be considered if the system applied for produce H₂ in small-scale. CO concentration gradually decreases until it almost drops to zero at higher R. Conversion of CH₄ is not affect by any value of R ratio.

In WGS reactors, more CO conversion occurs since more amount of water excess affect the H₂ formation. Thus, H₂ yield in WGS reactor of ATR system higher than SR system at the same R ratio. Furthermore, leaving stream from LWGS reactor consist of smaller amount of CO than SR system so H₂ is consumed a little in PrOX reactor and H₂ product stream does not leave at higher temperature.

5.2.2 Effect of preheating temperature

The variation of preheating temperature affects the reactor temperature of the ATR reactor, which is operated under adiabatic condition, since there is not the external heat transfer to the reactor and it also affects compositions of synthesis gas.

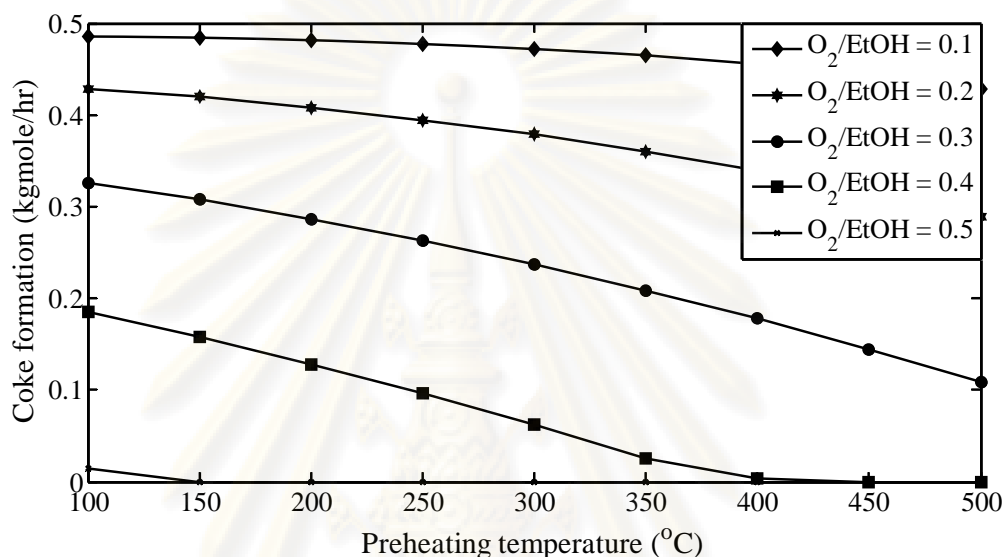


Fig. 5.9 Effect of preheating temperature on carbon formation in ATR reactor at $R = 1.5$ and 1 atm for each oxygen-to-ethanol molar ratio.

The result of carbon formation by varying preheating temperature at R ratio constant is depicted in Fig. 5.9. Carbon formation can be reduced by the increase of preheating temperature, however, only the increase of preheating temperature does not completely suppress carbon deposition at $O_2/EtOH$ molar ratio of below 0.4 in studied preheating temperature range of 100-500 °C. Furthermore, at higher $O_2/EtOH$ molar ratio, carbon is decreased by rising preheating temperature faster than at lower $O_2/EtOH$ molar ratio.

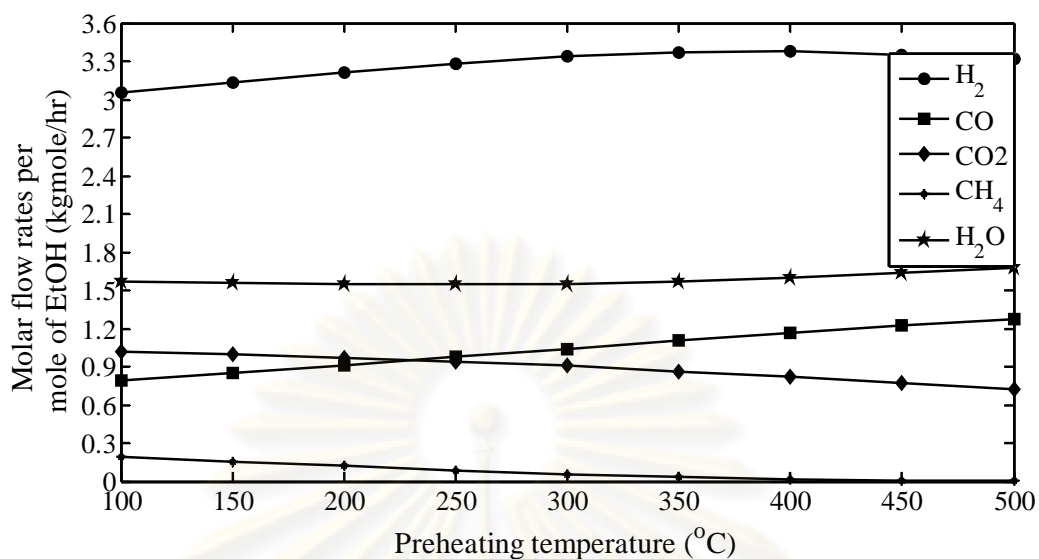


Fig. 5.10 Effect of preheating temperature on the equilibrium compositions in ATR reactor at oxygen-to-ethanol molar ratio = 0.7, $R = 2.0$ and 1 atm.

Fig. 5.10 presents the equilibrium compositions in ATR reactor as a function of preheating temperature at fixed $O_2/EtOH$ and R molar ratio. It is found that the equilibrium compositions in ATR reactor are dependent of preheating temperature. H_2 molar flow rate slightly increases to the maximum H_2 yield with increasing preheating temperature. CO molar flow rate also gradually increases, while the amount of CO_2 and CH_4 decreases when increasing preheating temperature. Unreacted H_2O , which remains in the reactor, is almost constant.

ศูนย์วิทยทรัพยากร
จุฬาลงกรณ์มหาวิทยาลัย

5.2.3 Effect of oxygen-to-ethanol molar ratio ($O_2/EtOH$)

$O_2/EtOH$ molar ratio significantly affects the adiabatic temperature that increases by supplying oxygen.

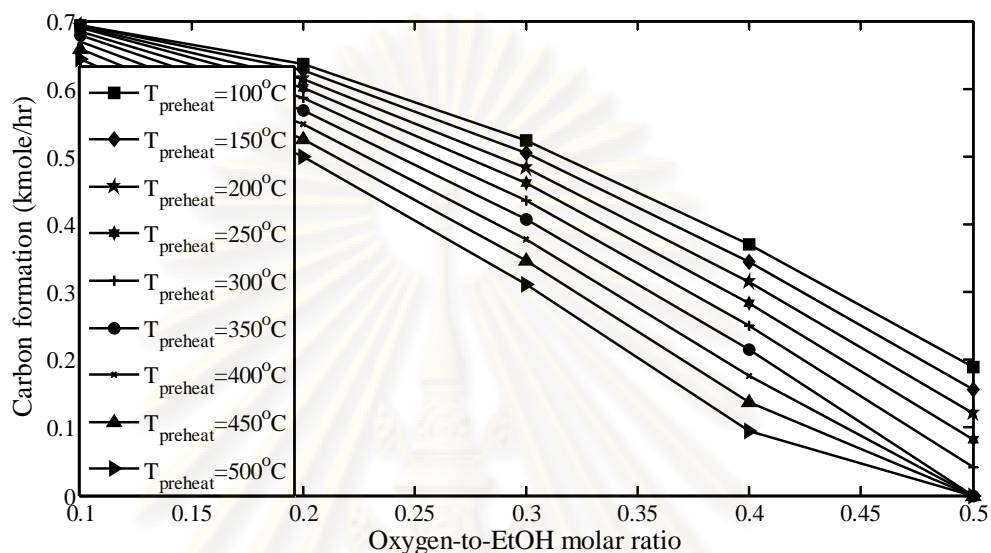


Fig. 5.11 Effect of oxygen-to-ethanol molar ratio on carbon formation in ATR reactor at $R = 1.0$ and 1 atm with preheating temperature in the range of 100 to 500 °C.

The effect of $O_2/EtOH$ molar ratio on the coking boundary is shown in Fig. 5.11. $O_2/EtOH$ molar ratio significantly affects the formation of carbon. It is generated at $O_2/EtOH$ molar ratio of less than 0.6 in ATR reactor with R of 1.0 and at 1 atm. At higher preheating temperature, carbon is suppressed faster than at lower preheating temperature.

ศูนย์วิทยทรัพยากร
จุฬาลงกรณ์มหาวิทยาลัย

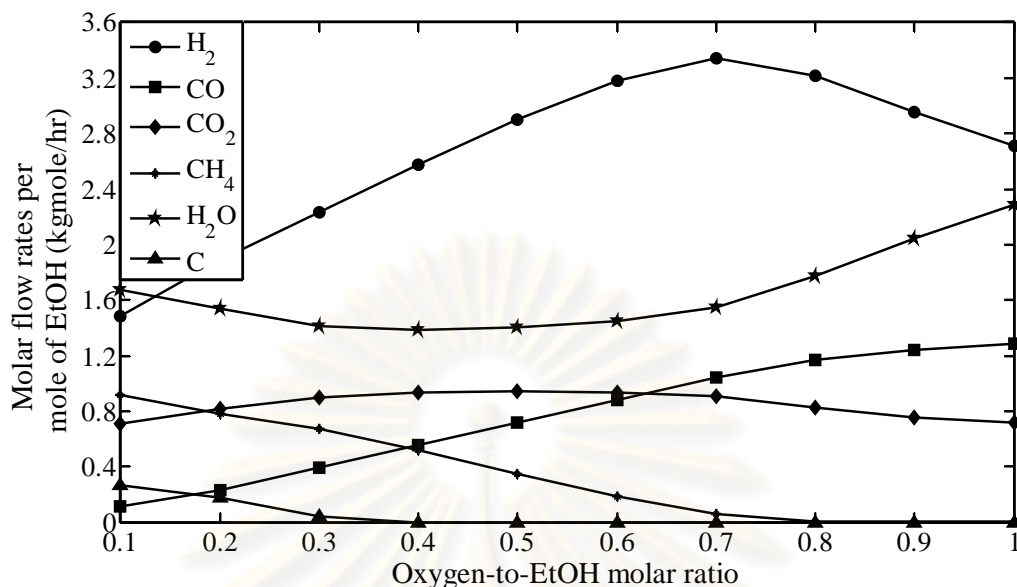


Fig. 5.12 Effect of oxygen-to-ethanol molar ratio on the equilibrium compositions in ATR reactor at $T_{\text{Preheat}} = 300\text{ }^{\circ}\text{C}$, $R = 2.0$ and 1 atm .

Fig 5.12 shows the results of the increase of O_2/EtOH , which is varied in the range of 0.1 to 1.0. At a fixed preheating temperature and pressure, H_2 concentration sharply increases to a peak with increasing O_2/EtOH molar ratio and then it reduces in the higher range of O_2/EtOH molar ratio due to the effect of excessive O_2 supply. CO_2 has the same trend like H_2 but it slower change than H_2 . Conversely, concentration of H_2O drops to minimum before it rises by increasing O_2/EtOH molar ratio. CO concentration increases in the O_2/EtOH molar ratio range of 0.1-1.0, while CH_4 and C slightly decrease and finally drop to zero.

Results of optimal water-to-EtOH molar ratio (R), preheating temperature and oxygen-to-EtOH molar ratio (O_2/EtOH) to generate maximum H_2 concentration under ATR adiabatic operation and no coke formation at pressure of 1 atm are summarized in table 5.2

จุฬาลงกรณ์มหาวิทยาลัย

Table 5.2 The optimum conditions of ATR reaction for maximizing hydrogen production under adiabatic conditions

Preheating temperature (°C)	Water-to-ethanol molar ratio ranges	Oxygen-to-ethanol molar ratio
100	0.5-4.5	0.8
	5.0-9.5	0.9
	10.0	1.0
200	0.5-10.0	0.8
300	0.5-10.0	0.7
400	0.5-2.0	0.7
	2.5-10.0	0.6
500	0.5	0.7
	1.0-5.0	0.6
	5.5-10.0	0.5

ศูนย์วิทยทรัพยากร
จุฬาลงกรณ์มหาวิทยาลัย

5.2.4 Analysis of autothermal reforming process

The product compositions of each reactor outlet are shown in Fig. 5.13. According to this graph maximum H_2 concentration generated from ATR system is about 36 mol% that is lower than SR system around 15 mol%, however, CO concentration generated from ATR reformer is lower than SR reformer at the same operating condition. So that there is a small amount of remaining CO entering PrOX reactor and H_2 is consumed a little. Moreover, it is found that the main diluent of H_2 product from ATR process is nitrogen.

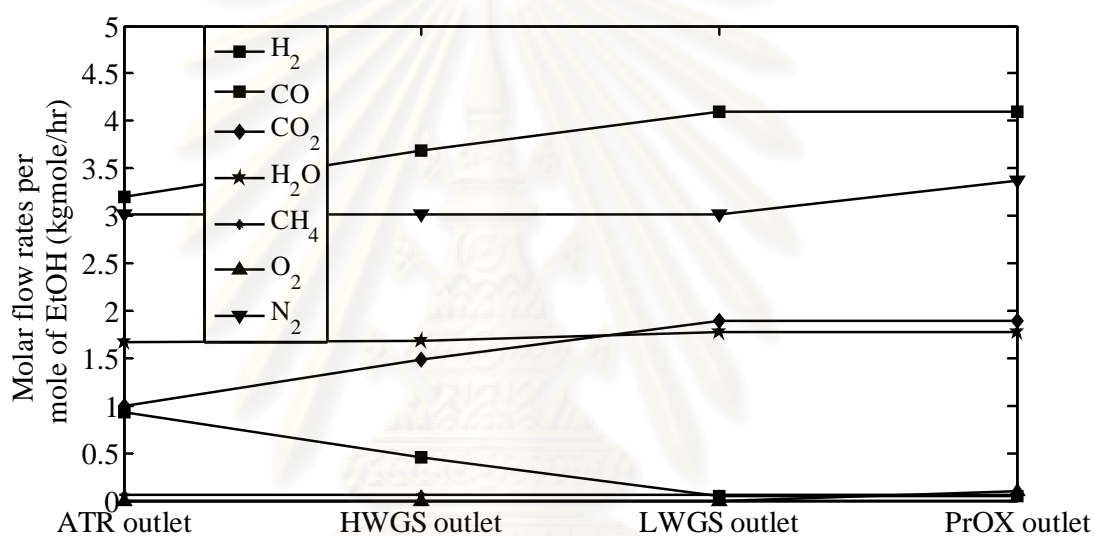


Fig. 5.13 The equilibrium compositions profile for autothermal reforming process at $R = 2.0$, $T_{Preheat} = 100\text{ }^\circ\text{C}$ and $P = 1\text{ atm}$.

5.3 Comparison between steam reforming and autothermal reforming of ethanol

Comparison of equilibrium composition from steam reforming and autothermal reforming reaction is determined separately in 2 cases. In the first case, the preheating temperature is fixed at $100\text{ }^\circ\text{C}$ ($T_{preheat} = 100\text{ }^\circ\text{C}$) and the reactor temperature is selected at an optimal value of steam reforming reaction for both reactions ($T_{ATR\text{ reactor}} = T_{SR\text{ reactor}}$). So oxygen is fed to autothermal reformer in order to supplying energy demand for preheating reactants and endothermic reaction at neutral energy condition, while steam reformer obtains energy required form external source. In the second case, steam reforming parameter is fixed as the first case. While, the both of the preheating and reactor temperature of ATR reaction are selected at the

optimal temperature of steam reforming ($T_{\text{preheat}} = T_{\text{ATR reactor}} = T_{\text{SR reactor}}$). So the oxygen ratio of autothermal reforming is fed to calculate the total amount of oxygen needed for endothermic reaction at neutral energy condition.

Fig. 5.14 shows the compared result of the first case by varying R ratio. In this studied case, O_2/EtOH feed ratio of ATR reaction is consumed for preheating reactants and endothermic reforming reaction.

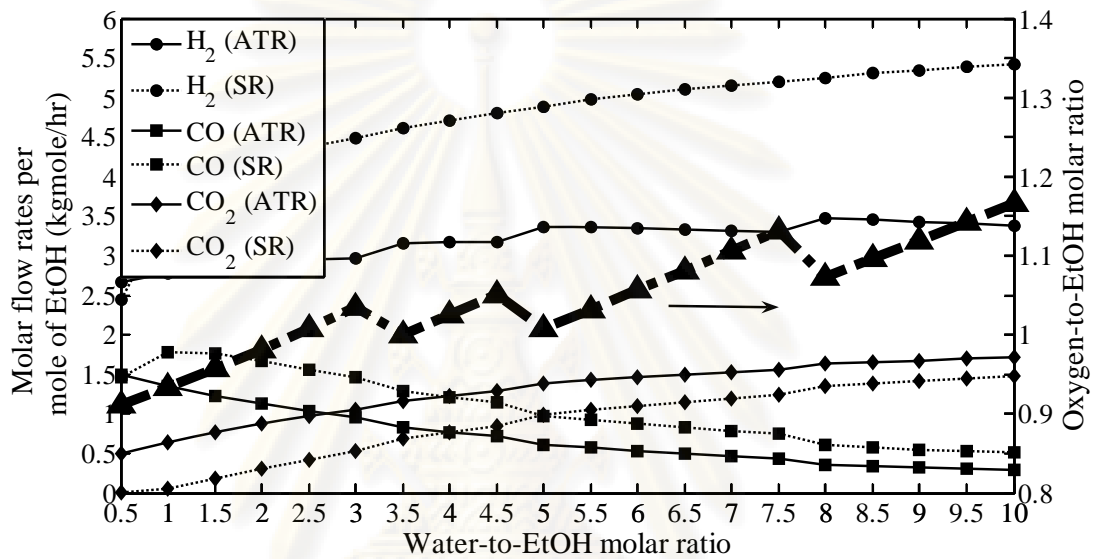


Fig. 5.14 Comparison of equilibrium compositions between steam reforming and autothermal reforming reaction at the preheating temperature = 100 °C and the optimal SR reactor temperature condition.

The observed trends in the product distribution in SR and ATR reaction are quite similar. The results show that SR reaction generates the amount of H_2 more than ATR reaction about 20-40 % concentration in R ratio range of 0.5-10.0. ATR reaction produces CO lower than SR reaction, however, CO_2 concentration from ATR reaction is higher than CO_2 from SR reaction. The different of the amount of CO and CO_2 between SR and ATR decrease when R ratio increases. The O_2/EtOH consumption increases as R ratio rises since the preheating of water requires more the energy supplied.

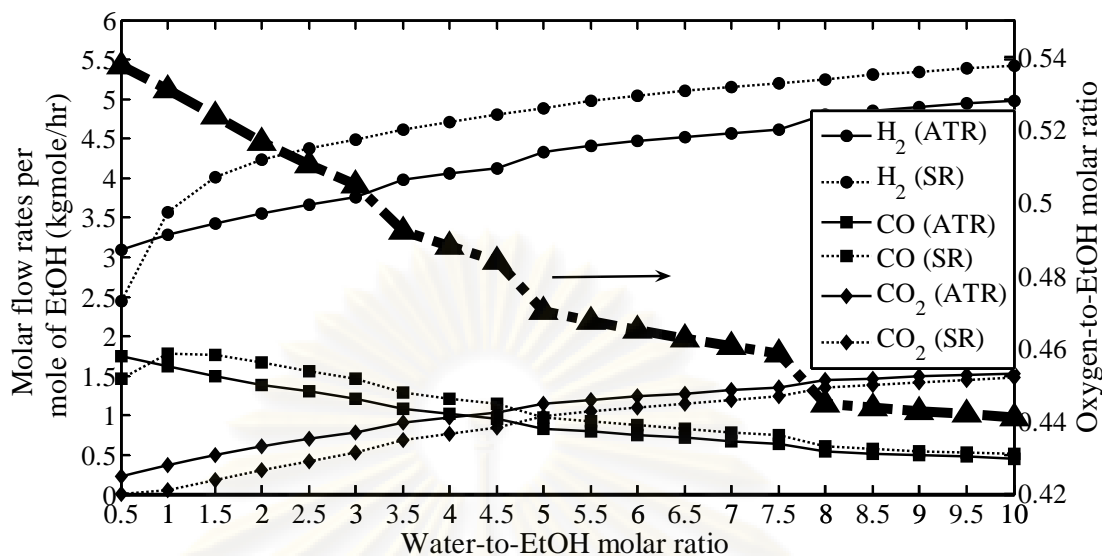


Fig. 5.15 Comparison of equilibrium compositions between steam reforming reaction at the optimal SR reactor temperature and autothermal reforming reaction at the same temperature of preheating and reactor.

Fig. 5.15 presents the product distribution when the preheating and reactor temperature of ATR reaction equal steam reforming optimal temperature. In this studied case, O₂/EtOH consumed value is used to investigate the amount of necessary heat for the endothermic reforming reaction. It is found that the O₂/EtOH consumption decreases with increasing of R ratio and its value is required lower than the first case. The trend of product distribution is similar the first case result. It shows that H₂ concentration from ATR reaction lower than from SR reaction around 10-15 % concentration. The different of the amount of CO and CO₂ between SR and ATR is smaller than the first case. Moreover, their concentrations are almost equally generated at high value of R ratio.

5.4 CO₂ capture section

The effect of main parameters consisting of MEA concentration, circulation rate, number of absorber and stripper stages and temperature of absorber inlet on the CO₂ scrubbing process is investigated by keeping the other parameters constant. Leaving gas stream from LWGS reactor is cooled in order to condense some water before entering the CO₂ capture method at selected inlet gas temperature.

5.4.1 Effect of MEA concentration

Typical solution concentration for MEA is in the range of 15-30 wt%. In this studied case, the effect of MEA concentration on purity of H₂ and CO₂ removal is investigated by varying MEA concentration in solution lower than 30 wt%. Inlet gas obtains from steam reforming and shift reactor with R ratio of 2.5. The composition of inlet gas and the other parameters is shown in table 5.3.

Table 5.3 Flow component of inlet gas and assumption for MEA concentration modeled case.

Inlet gas temperature	40 °C	Number of absorber stages	10
Inlet gas composition		Lean amine temperature	40 °C
H ₂ O (kgmole/hr)	0.6145	Circulation rate (kgmole/hr)	45.0000
H ₂ (kgmole/hr)	5.8598	Number of stripper stages	15
CO (kgmole/hr)	8.010E-2	Pressure system	1 atm
CO ₂ (kgmole/hr)	1.9047		
CH ₄ (kgmole/hr)	1.503E-2		
Total flow (kgmole/hr)	8.4741		

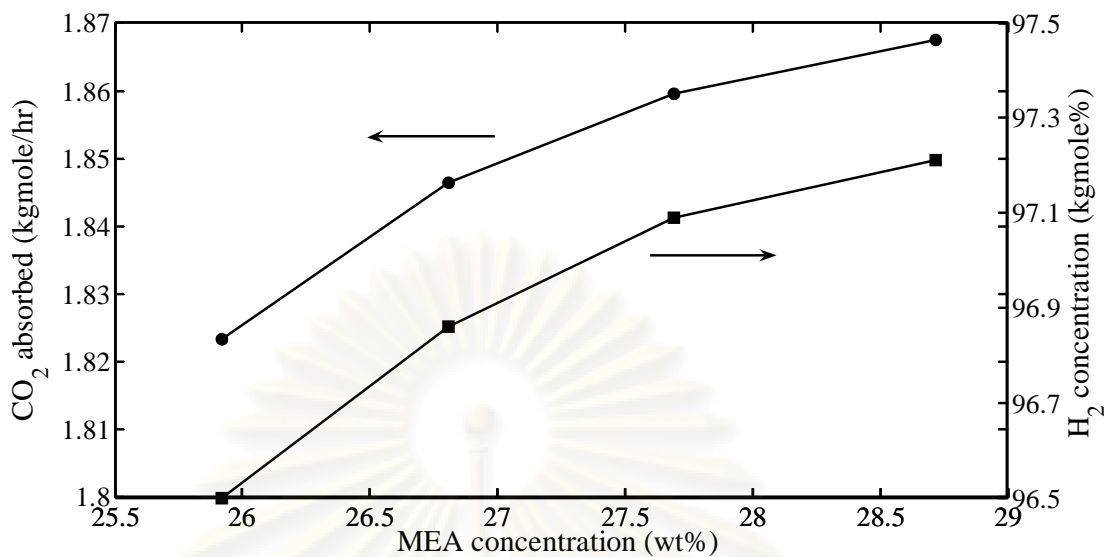


Fig. 5.16 Effect of MEA concentration on CO₂ absorbed concentration and the purity of H₂.

From Fig 5.16, variation of MEA concentration is found that higher MEA concentration can absorb more CO₂ than the lower concentration when the circulation rate is fixed. Besides, this result affects the purity of H₂ product that is highest about 97 mol% but the main drawback of higher MEA concentration is the increase of corrosion when the concentration is higher than 20 wt%. This corrosion can also affect to reduce the quality of amine solvent.

5.4.2 Effect of circulation rate

The effect of circulation rate is calculated to indicate the recovered CO₂ grade, the purity of H₂ product and the heat consumption in the reboiler. Inlet gas obtains from steam reforming and shift reactor with R ratio of 2.5. The composition of inlet gas and the other parameters is shown in table 5.4.

Table 5.4 Flow component of inlet gas and assumption for CO₂ capture circulation rate modeled case

Inlet gas temperature	40 °C	Number of absorber stages	10
Inlet gas composition		Lean amine temperature	40 °C
H ₂ O (kgmole/hr)	0.6145	MEA in lean amine	26 wt%
H ₂ (kgmole/hr)	5.8598	Number of stripper stages	15
CO (kgmole/hr)	8.010E-2	Pressure system	1 atm
CO ₂ (kgmole/hr)	1.9047		
CH ₄ (kgmole/hr)	1.503E-2		
Total flow (kgmole/hr)	8.4741		

The circulation rate is varied in the range of 45-72 kgmole/hr and the results are presented in Fig. 5.17-5.18. From Fig. 5.17, the increase of circulation rate results in the increase of CO₂ absorbed concentration and purity of H₂ product. However, the reboiler requires more consumption of heat energy due to the increase of amine solution. The increase of CO₂ removal concentration also results from heat consumption rising (See Fig. 5.18). Therefore, low circulation rate demands minimum heat consumption.

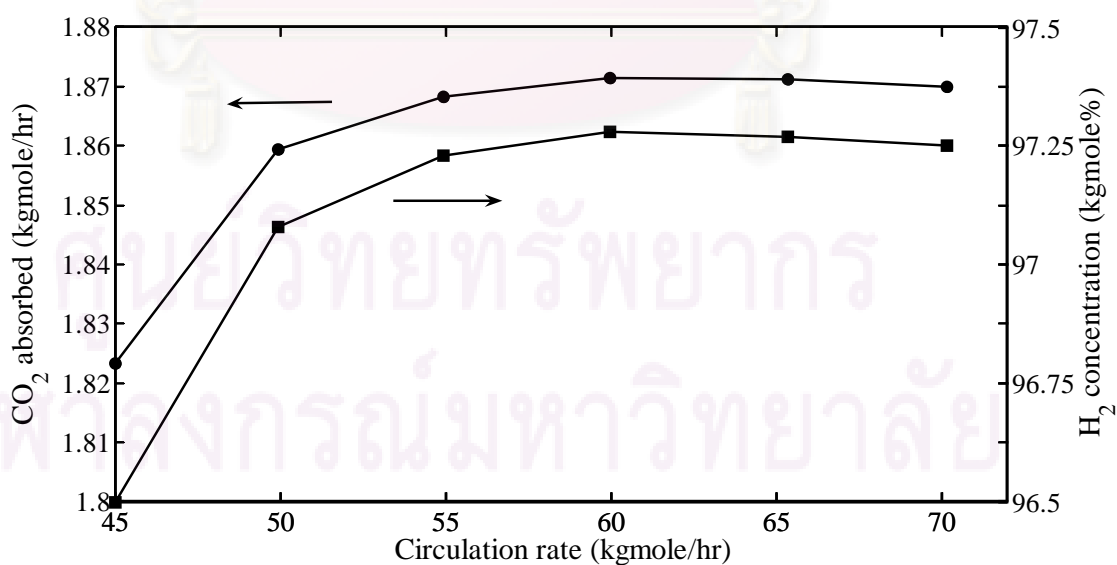


Fig. 5.17 Effect of circulation rate on CO₂ absorbed concentration and the purity of H₂.

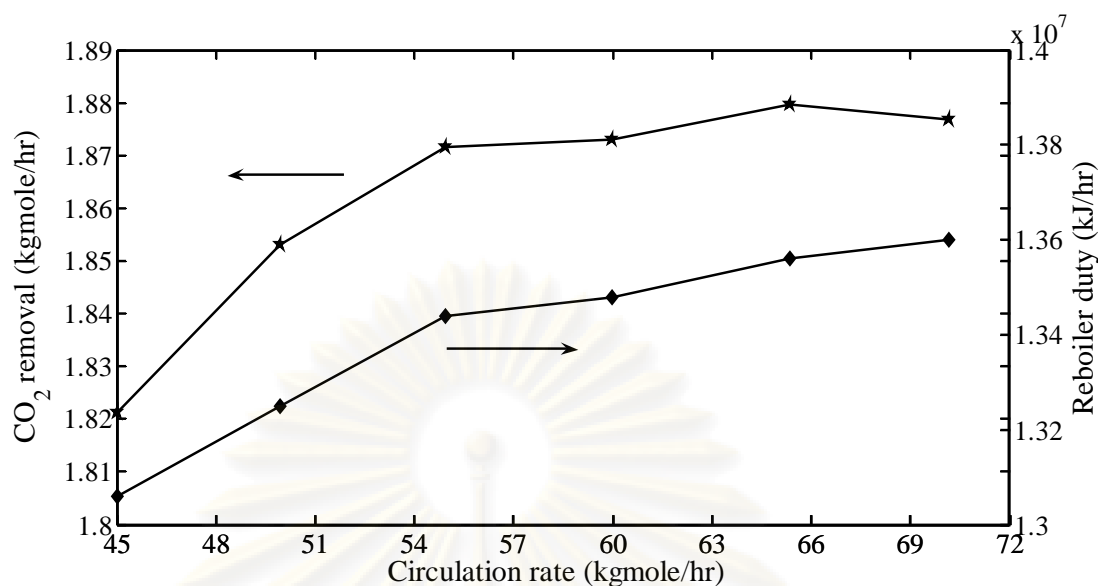


Fig. 5.18 Effect of circulation rate on CO₂ removal and reboiler duty.

5.4.3 Effect of number of stages

Number of absorber and stripper stages significantly affects the amount of CO₂ absorbed and CO₂ removal, purity of H₂ product and reboiler duty. First, number of absorber stages is calculated with inlet gas at R of 2.5. The flow component of inlet gas and defined parameter is shown in table 5.5.

Table 5.5 Flow component of inlet gas and assumption for absorber stages modeled case

Inlet gas temperature	40 °C	Lean amine temperature	40 °C
Inlet gas composition		MEA in lean amine	26 wt%
H ₂ O (kgmole/hr)	0.6145	Circulation rate (kgmole/hr)	46.0000
H ₂ (kgmole/hr)	5.8598	Number of stripper stages	10
CO (kgmole/hr)	8.010E-2	Pressure system	1 atm
CO ₂ (kgmole/hr)	1.9047		
CH ₄ (kgmole/hr)	1.503E-2		
Total flow (kgmole/hr)	8.4741		

The result of number of absorber stages variation is shown in Fig. 5.19-5.20. The amount of CO₂ absorbed and CO₂ removal, purity of H₂ product and reboiler duty increase by increasing number of absorber stages that is varied from 4 to 14.

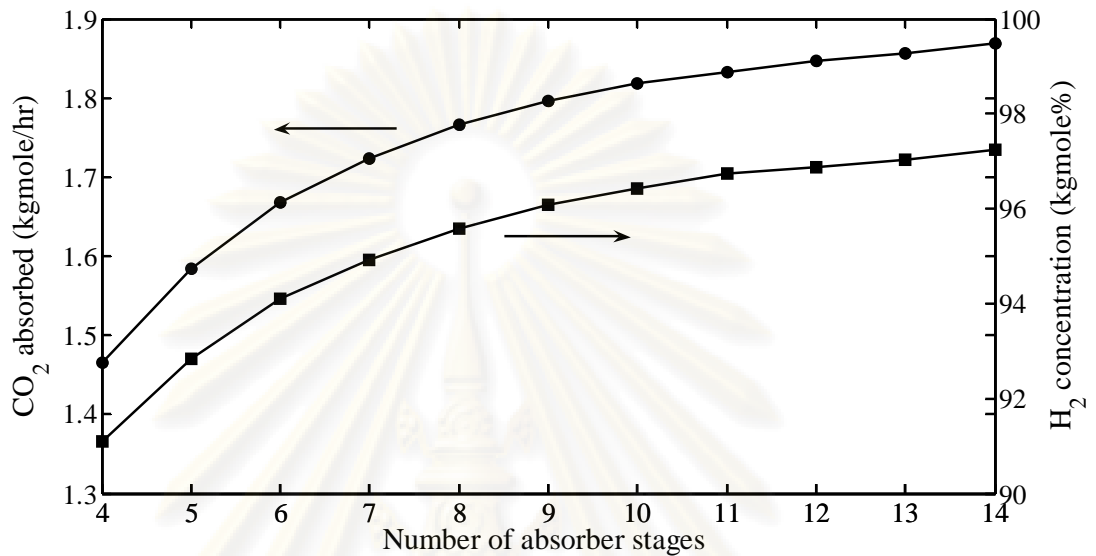


Fig. 5.19 Effect of number of absorber stages on CO₂ absorbed concentration and the purity of H₂ product.

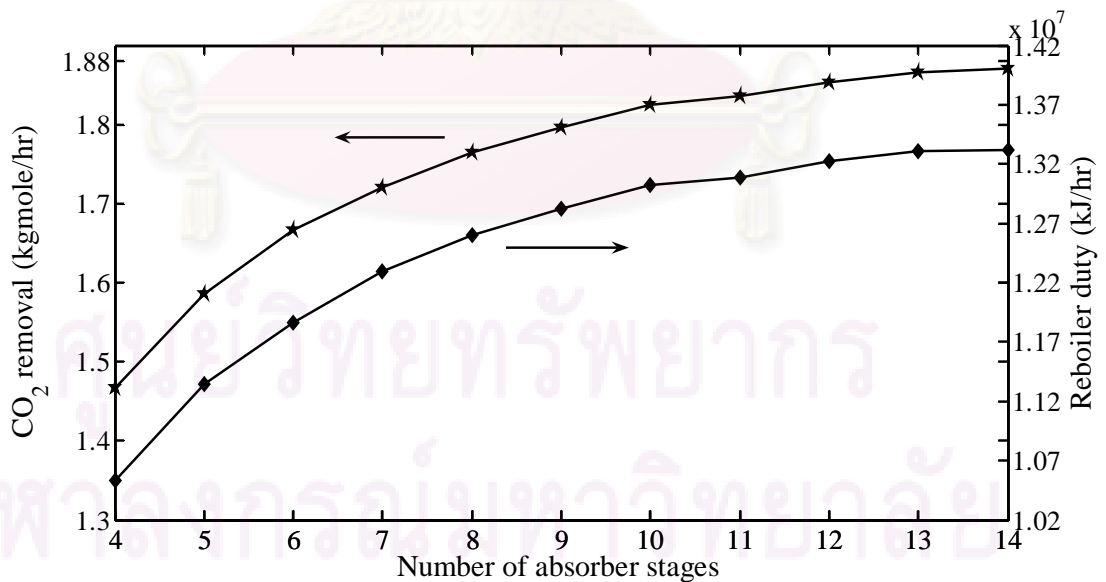


Fig. 5.20 Effect of number of absorber stages on CO₂ removal and reboiler duty.

Number of stripper stages is also calculated with inlet gas at R of 2.5. The composition of inlet gas and the other parameters is shown in table 5.6.

Table 5.6 Flow component of inlet gas and assumption for absorber stages modeled case

Inlet gas temperature	40 °C	Number of absorber stages	10
Inlet gas composition		Lean amine temperature	40 °C
H ₂ O (kgmole/hr)	0.6145	MEA in lean amine	26 wt%
H ₂ (kgmole/hr)	5.8598	Circulation rate (kgmole/hr)	45.6000
CO (kgmole/hr)	8.010E-2	Pressure system	1 atm
CO ₂ (kgmole/hr)	1.9047		
CH ₄ (kgmole/hr)	1.503E-2		
Total flow (kgmole/hr)	8.4741		

Number of stripper stages is varied from 8 to 18 and the data is presented in Fig. 5.21-5.22. The result of changing the number of stripper stages has the same tendency as changing the number of absorber stages, however, the variation of stripper stages required lower heat consumption than the variation of absorber stages at the same CO₂ removal.

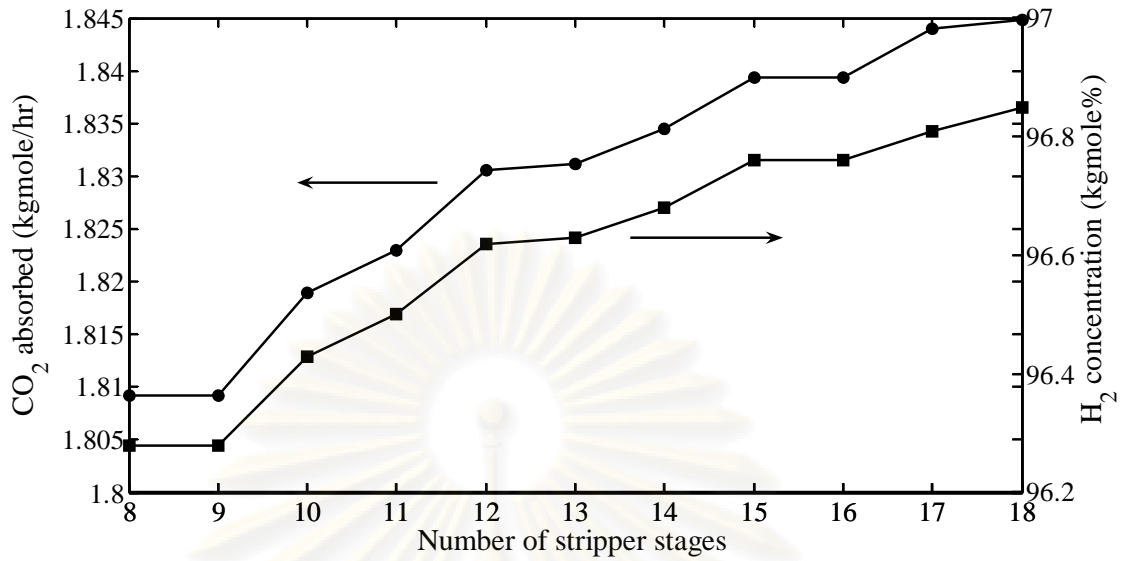


Fig. 5.21 Effect of number of stripper stages on CO₂ absorbed concentration and the purity of H₂ product.

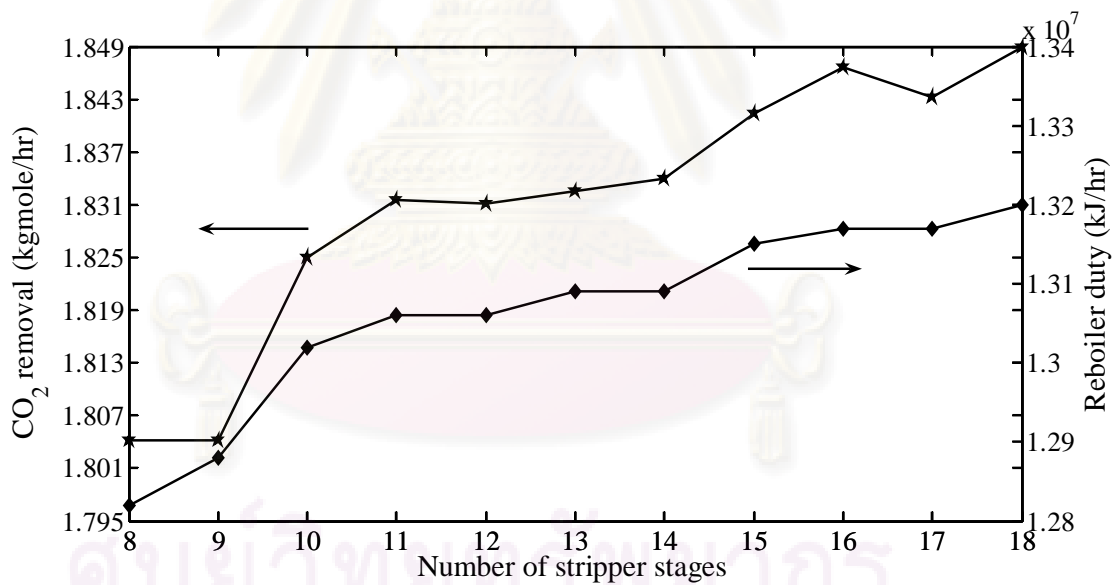


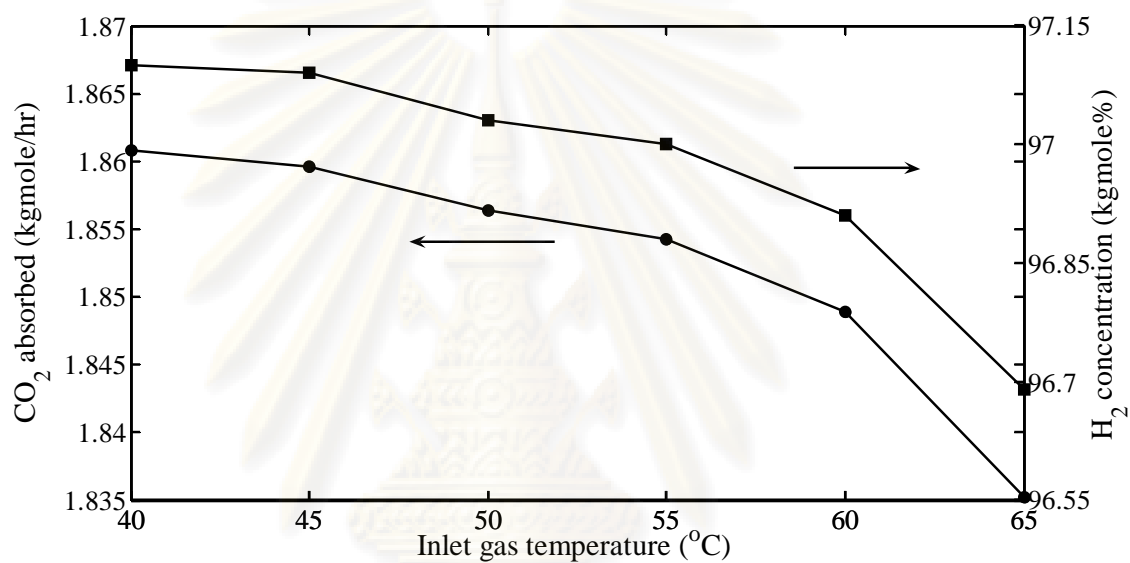
Fig. 5.22 Effect of number of stripper stages on CO₂ removal and reboiler duty.

5.4.4 Effect of inlet gas temperature

After leaving water gas shift reactor, the synthesis gas is cooled at selected temperature in the range of 40-65 °C before entering separator unit in order to condense some water from the gas stream. Thus, there are minor variations in inlet gas compositions

Table 5.7 The assumption for absorber inlet gas temperature modeled case

Number of absorber stages	10
MEA in lean amine	26 wt%
Circulation rate (kgmole/hr)	50.0000
Number of stripper stages	15
Pressure system	1 atm

**Fig. 5.23** Effect of absorber inlet gas temperature on CO₂ absorbed concentration and the purity of H₂.

ศูนย์วิทยทรัพยากร
จุฬาลงกรณ์มหาวิทยาลัย

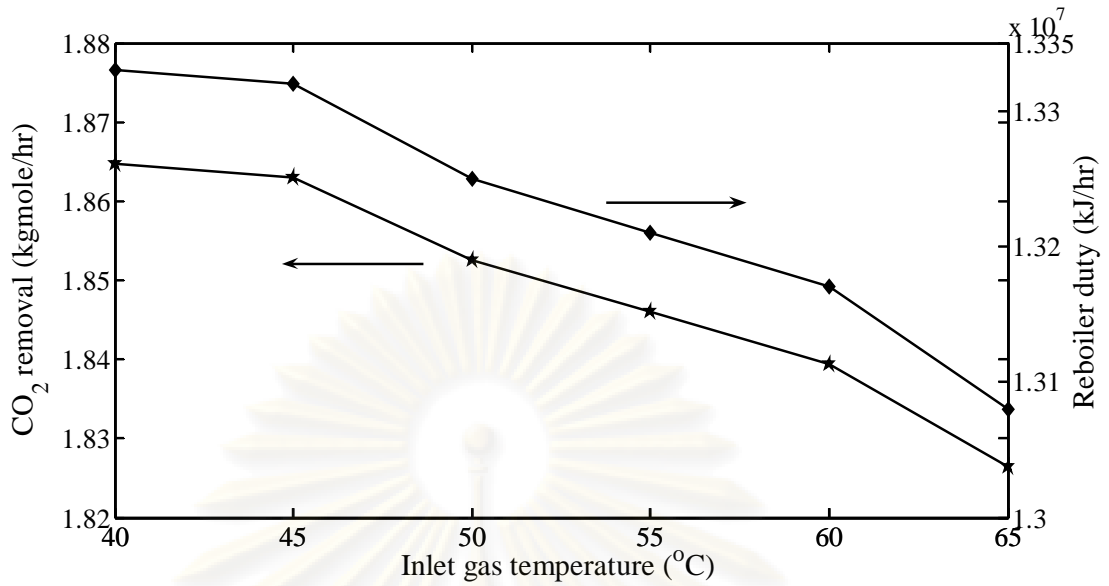


Fig. 5.24 Effect of absorber inlet gas temperature CO₂ removal and reboiler duty.

The difference of absorber inlet gas temperature has influence on product purity and reboiler duty. The inlet temperature variation is presented in Fig. 5.23-5.24 by fixing the other parameters that is shown in table 5.7. The results show that the increase of inlet temperature can cause decreases in CO₂ absorbed concentration, CO₂ removal, purity of H₂ and reboiler duty.

CHAPTER VI

CONCLUSIONS

In this study, the thermodynamic characteristics of the reforming process including, steam reforming and autothermal reforming of ethanol for hydrogen production is investigated by using HYSYS simulation software. Each reforming reactor is identified its own favorable operating conditions for hydrogen production with high yield and no coke formation.

The effect of operating parameters i.e., water-to-ethanol molar ratio and operating temperature on the performance of a steam reforming process affect to the amount and concentration of hydrogen, carbon monoxide, carbon dioxide and methane in gaseous mixture. It is found that at the specified water-to-ethanol molar ratio, there is an optimal operating temperature of the reformer maximizing the yield of hydrogen. The overall efficiency of hydrogen production process increases with increasing water-to-ethanol molar ratio, however, more heat energy is required for the steam reformer in order to vaporize the amount of water input. Besides, the deposition of carbon in reformer can be removed by increasing the ratio of water-to-EtOH and temperature. A preheat of the reformer feed using the heat integration process can reduce an external heat required for steam reforming reaction.

Thermodynamic equilibrium of autothermal reforming reaction is studied as a function of water-to-ethanol molar ratio, oxygen-to-ethanol and preheating temperature under adiabatic condition. The product compositions are examined, including the coking boundary. In this reaction, oxygen is fed to generate energy by the oxidation reaction in order to compensate the energy absorbed by reforming endothermic reaction.

The results show that coke deposition is limited at water-to-ethanol molar ratio lower than 3.0 and preheating temperature also affects to suppress carbon, however, water-to-ethanol molar ratio significantly affects the formation of carbon more than preheating temperature. At a fixed oxygen ratio and preheating temperature, hydrogen molar flow rate increases as water ratio rises but at higher water ratio, it achieves an almost constant value.

Preheating temperature significantly affects to oxygen ratio parameter due to a higher preheating temperature can reduce oxygen required for preheating reactants and supplying the endothermic reaction in the reformer. Under adiabatic condition, the maximum hydrogen yield is achieved at an optimal oxygen-to-ethanol molar ratio with constant of other operating parameters.

In the first case of the product distribution comparison between steam reforming and autothermal reforming is found that steam reforming generates more hydrogen concentration than autothermal reforming at the same operating conditions. Furthermore, the oxygen consumption increases by rising water ratio due to the increase of the heat consumed in water evaporation.

In the second case of the product distribution comparison between steam reforming and autothermal reforming results in the decrease of oxygen consumption and the amount of hydrogen generated from autothermal reforming reaction is higher than the first case due to the decrease of heat demanded from oxidation reaction.

The carbon dioxide capture model is studied the effect of using monoethanolamine (MEA) as solvent on the purification process. The main parameters consisting of circulation rate, number of absorber and stripper stages and temperature of absorber inlet significantly affect to recovery of carbon dioxide and heat consumption in reboiler. The increase of carbon dioxide removal results from increasing of absorber and stripper stage, however, it demand high heat consumption. This process can purify hydrogen product stream from steam reforming system up to about 97 mol%.

REFERENCES

- Adhikaria, S.; Fernandoa S.; Gwaltneyb, S.R.; Toa, S.D.F.; Brickac, R.M.; Steele, P.H.; and Haryantoa A. A thermodynamic analysis of hydrogen production by steam reforming of glycerol. International Journal of Hydrogen Energy 32 (2007): 2875 – 2880.
- Ahmed, I. and Gupta, A.K. Evolution of syngas from cardboard gasification. Applied Energy 86 (2009): 1732-1740.
- Akande, A.; Aboudheir, A.; Idem, R.; and Dalai, A. Kinetic modeling of hydrogen production by the catalytic reforming of crude ethanol over a co-precipitated Ni-Al₂O₃ catalyst in a packed bed tubular reactor. International Journal of Hydrogen Energy 31 (2006): 1707–1715.
- Alie, C.; Backham, L.; Croiset, E.; and Douglas, P.L. Simulation of CO₂ capture using MEA scrubbing: a flowsheet decomposition method. Energy Conversion and Management 46 (2005): 475-487.
- Anderson, R.B. The Fischer-Tropsch Synthesis. Academic Press, INC., 1984.
- Balzhiser, S.E. Chemical Engineering Thermodynamics. PRENTICE-HALL International, 1972.
- Barbier, J. Coking of reforming catalysts. Catalyst Deactivation (1987): 1.
- Benito, M.; Sanz, J.L.; Isabel, R.; Padilla R.; Arjona, R.; and Daza, L. Bio-ethanol steam reforming: Insights on the mechanism for hydrogen production. Journal of Power Sources 151 (2005): 11-17.
- Benito, M.; Padilla, R.; Sanz, J.L.; and Daza, L. Thermodynamic analysis and performance of a 1 kW bioethanol processor for a PEMFC operation. Journal of Power Sources 169 (2007): 123-130.
- Biswas, J.; Gray, P.G.; and Do, D.D. The reformer lineout phenomenon and its fundamental importance to catalyst deactivation. Applied Catalysis 32 (1987): 249-274.
- Brown, L.F. A comparative study of fuels for on-board hydrogen production for fuel-cell-powered automobiles. International Journal of Hydrogen Energy 26 (2001): 381-397.

- Bualom Jaikaew. Effect of alkali metals in dehydrogenation catalysts for coke reduction. Master's Thesis, Department of Chemical Engineering, Graduated School, Chulalongkorn University, 1995.
- Choi, Y., and Stenger, H. G. Kinetics, simulation and insights for CO selective oxidation in fuel cell applications. Journal of Power Sources 129 (2004): 246-254.
- Choi, Y., and Stenger, H.G. Water gas shift reaction kinetics and reactor modeling for fuel cell grade hydrogen. Journal of Power Sources 124 (2003): 432–439.
- Coulson, J.M.; Richardson, J.F.; and Sinnott, R.K. Chemical Engineering. Vol. 6. Pergamon Press, 1983.
- Darwish, N.A.; Hilal, N.; Versteeg, G.; and Heesink, B. Feasibility of the direct generation of hydrogen for fuel-cell-powered vehicles by on board steam reforming of naphtha. Fuel 83 (2004): 409-417.
- Ersoz, A. Investigation of hydrocarbon reforming process for micro-cogeneration systems. International Journal of Hydrogen Energy 33 (2008): 7084-7094.
- Ersoz, A.; Olgun, H.; Ozdogan, S.; Gungor, C.; Akgun, F.; and Tiris, M. Autothermal reforming as a hydrocarbon fuel processing option for PEM fuel cell. Journal of Power Sources 118 (2003): 384-392.
- Francesconi, J.A. ; Mussati, M.C. ; Mato, R.O. ; and Aguirre, P.A. Analysis of the energy efficiency of an integrated ethanol processor for PEM fuel cell systems. Journal of Power Sources 167 (2007): 151-161.
- Giunta, P.; Mosquera, C.; Amadeo, N.; and Laborde, M. Simulation of a hydrogen production and purification system for a PEM fuel-cell using bioethanol as raw material. Journal of Power Sources 164 (2007): 336-343.
- Gökalliler, F.; Caglayan, B.S.; Önsan, Z.İ.; and Aksoylu, A.E. Hydrogen production by autothermal reforming of LPG for PEM fuel cell applications. International Journal of Hydrogen Energy 33 (2008): 1383-1391.
- Hohn, K.L., and DuBois, T. Simulation of a fuel reforming system based on catalytic partial oxidation. Journal of Power Sources 183 (2008): 295-302.
- Huang, C., and T-Raissi, A. Analyses of one-step liquid hydrogen production from methane and landfill gas. Journal of Power Sources 173 (2007): 950-958.
- Lyubovsky, M., and Walsh, D. Reforming system for co-generation of hydrogen and mechanical work. Journal of Power Sources 157 (2006): 430-437.

- Jeom, I.B.; Ji, H.Y.; and Hee, M.E. Prediction of equilibrium solubility of carbon dioxide in aqueous 2-amino-2-methyl-1,3-propanediol solutions. Korean Journal of Chemical Engineering 17(4) (2000): 484-487.
- Kent, R.L., and Eisenberg, B. Better data for amine treating. Hydrocarbon Process 55 (1976): 87.
- Li, M.-H., and Shen, K.-P. Calculation of equilibrium solubility of carbon dioxide in aqueous mixtures of monoethanolamine with methyldiethanolamine. Fluid Phase Equilibria 85 (1993): 129.
- Li, Y.; Wang, Y.; Zhang, X.; and Mi, Z. Thermodynamic analysis of autothermal steam and CO₂ reforming of methane. International Journal of Hydrogen Energy 33 (2008): 2507–2514.
- Lwin, Y.; Ramli, W.D.; Mohamad, A.B.; and Yaakob, Z. Hydrogen production from steam-methanol reforming: thermodynamic analysis. International Journal of Hydrogen Energy 25 (2000): 47–53.
- Lyubovsky, M., and Walsh, D. A reforming system for co-generation of hydrogen and mechanical work from methanol. Journal of Power Sources 162 (2006): 597-605.
- Lyubovsky, M., and Walsh, D. Reforming system for co-generation of hydrogen and mechanical work. Journal of Power Sources 157 (2006): 430-437.
- Mieville, R.L. Coking kinetics of reforming. Catalyst Deactivation. (1991): 151-159.
- Mofarahi, M.; Khojasteh, Y.; Khaledi, H.; and Farahnak, A. Design of CO₂ absorption plant for recovery of CO₂ from flue gases of gas turbine. Energy 33 (2008): 1311-1319.
- Narong Lim. Effect of promoters on coke formation on metal site of propane dehydrogenation catalyst. Master's Thesis, Department of Chemical Engineering, Graduated School, Chulalongkorn University 1996.
- Ni, M.; Leung, D.Y.C.; and Leung, M.K.H. A review on reforming bio-ethanol for hydrogen production. International Journal of Hydrogen Energy 32 (2007): 3238-3247.
- Peng, D.Y., and Robinson, D.B. A new two-constant equation of state. Industrial and Engineering Chemistry: Fundamentals 15 (1976): 59–64.
- Perna, A. Hydrogen from ethanol: Theoretical optimization of a PEMFC system integrated with a steam reforming Processor. International Journal of Hydrogen Energy 32 (2007): 1811-1819.

- Piniy Reargmuang. Absorber design program for hydrochloric vapor, Master's Thesis, Department of Chemical Engineering, Graduated School, Chulalongkorn University 1997.
- Qi, A.; Wang, S.; Fu, G.; and Wu, D. Autothermal reforming of n-octane on Ru-based catalysts. Applied Catalysis A General 293 (2005): 71–82.
- Semelsberger, T.A.; Brown, L.F.; Borup, R.L.; and Inbody, M.A. Equilibrium products from autothermal processes hydrogen-rich fuel-cell feeds. International Journal of Hydrogen Energy 29 (2004): 1047-1064.
- Seo, Y.-S.; Shirley, A.; and Kolaczkowski, S.T. Evaluation of thermodynamically favourable operating conditions for production of hydrogen in three different reforming technologies. Journal of Power Sources 108 (2002): 213-225.
- Solli, C.; Anantharaman, R.; Strømman, A.H.; Zhang, X.; and Hertwich, E.G. Evaluation of different CHP options for refinery integration in the context of a low carbon future. International Journal of Greenhouse Gas Control 3 (2009): 152-160.
- Tanabe, K.; Misono, M.; Ono, Y.; and Hattori, H. New solid acids and bases, Their catalytic properties, Studies in surface science and catalyst. Elsevier, Amsterdam, 51 (1989): 340-341.
- Tourneux, D.L.; Iliuta, I.; Iliuta, M.C.; Fradette, S.; and Larachi, F. Solubility of carbon dioxide in aqueous solutions of 2-amino-2-hydroxymethyl-1,3-propanediol. Fluid Phase Equilibria 268 (2008): 121-129.
- Vagia, E. Ch., and Lemonidou, A.A. Thermodynamic analysis of hydrogen production via autothermal steam reforming of selected components of aqueous bio-oil fraction. International Journal of Hydrogen Energy 33 (2008): 2489–2500.
- Wang, She., and Wang, Shu. Thermodynamic equilibrium composition analysis of methanol autothermal reforming for proton exchanger membrane fuel cell based on FLUENT Software. Journal of Power Sources 185 (2008): 451–458.
- Wilhem, D.J.; Simbeck, D.R.; Karp, A.D.; and Dickenson, R.L. Syngas production for gas-to-liquids applications: technologies, issues and outlook. Fuel Processing Technology 71 (2001): 139-148.
- Zalc, J.M., and Löffler, D.G. Fuel processing for PEM fuel cells: transport and kinetic issues of system design. Journal of Power Sources 111 (2002): 58–64.



APPENDICES

ศูนย์วิทยทรัพยากร
จุฬาลงกรณ์มหาวิทยาลัย

APPENDIX A

THERMODYNAMIC PROPERTY PACKAGE

In order to determine gas composition obtained from a reforming process for hydrogen production, thermodynamic property package have to be specified. In this study, equilibrium gas compositions are calculated using Peng-Robinson equation of state as a fluid package. The Peng-Robinson equation of state is generally the recommended property package for the system containing hydrocarbons, water, air, and combustion gases and can be expressed as follows:

$$p = \frac{RT}{V_m - b} - \frac{a\alpha}{V_m^2 + 2bV_m - b^2} \quad (\text{A.1})$$

where $a = \frac{0.45724R^2T_c^2}{p_c}$

$$b = \frac{0.07780RT_c}{p_c}$$

$$\alpha = \left[1 + (0.37464 + 1.54226\omega - 0.26992\omega^2)(1 - T_r^{0.5}) \right]^2$$

$$T_r = \frac{T}{T_c}$$

Alternatively, the Peng-Robinson equation of state can be given in polynomial form as shown below:

$$Z^3 - (1 - B)Z^2 + (A - 3B^2 - 2B)Z - (AB - B^2 - B^3) = 0 \quad (\text{A.2})$$

where $A = \frac{a\alpha p}{R^2T^2}$

$$B = \frac{bp}{RT}$$

The Peng-Robinson equation was developed in 1976 in order to satisfy the following goals (Peng et al., 1976):

1. The parameter should be expressible in terms of the critical properties and the acentric factor .

2. The model should provide reasonable accuracy near the critical point, particularly for calculations of the compressibility factor and liquid density.

3. The mixing rules should not employ more than a single binary interaction parameter, which should be independent of temperature pressure and composition.

Although most parts appeared in the Peng-Robinson equation are similar to the Soave equation, it is generally superior in predicting the liquid densities of many materials, especially nonpolar ones.



ศูนย์วิทยทรัพยากร
จุฬาลงกรณ์มหาวิทยาลัย

APPENDIX B

MONOETHANOLAMINE PROPERTY

Monoethanolamine (MEA) in aqueous solution is used for scrubbing acid gases in amine treaters. The aqueous solution of MEA acting as a weak base neutralizes acidic compounds dissolved in the solution to turn the molecules into an ionic form, making them polar and considerably more soluble in a cold MEA solution.

Table B.1 Monoethanolamine property

Molecular formula	C ₂ H ₇ NO
Molecular structure	$ \begin{array}{c} \diagup \text{C} \text{ --- } \text{C} \text{ --- } \text{OH} \\ \text{N} \text{ --- } \text{H} \\ \diagdown \text{H} \end{array} $
Molar mass (g/mole)	61.08
Density (g/ cm ³)	1.012
Melting point (°C)	10.3
Boiling point (°C)	170
Solubility in water	Miscible

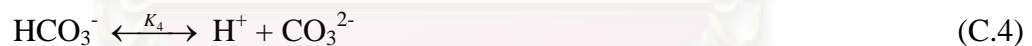
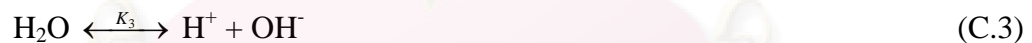
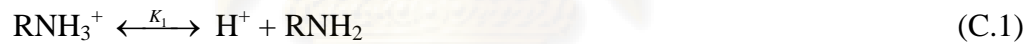
ศูนย์วิทยทรัพยากร
จุฬาลงกรณ์มหาวิทยาลัย

APPENDIX C

SOLUABILITY OF CO₂ IN AMINE SOLUTION

Kent and Eisenberg (1976) developed a simple thermodynamic for predicting equilibrium data in amine–CO₂ systems using apparent equilibrium constants. The Kent–Eisenberg model was chosen in this work because it yields a good performance for the correlation and prediction of CO₂ solubility in alkanolamine solutions as reported in several previous studies (Li et al., 1993; Jeom et al., 2000). The model is based on several equilibrium constants and the Henry's law relationship. The simplicity of the Kent and Eisenberg model lies in the fact that only the equilibrium constants involving the target amine are determined by fitting the measured gas solubility data while using the carbonic acid and water equilibrium constants as well as Henry's law constants (Tourneux et al., 2008).

The equilibrium reaction of carbon dioxide with aqueous solution of amine is assumed as follows (Jeom et al., 2000):



Each of the above reactions is characterized by a thermodynamically constant K_i according to the following expressions:

$$K_1 = \frac{[\text{H}^+][\text{RNH}_2]}{[\text{RNH}_3^+]} \quad (\text{C.5})$$

$$K_2 = \frac{[\text{H}^+][\text{HCO}_3^-]}{[\text{H}_2\text{O}][\text{CO}_2]} \quad (\text{C.6})$$

$$K_3 = \frac{[\text{H}^+][\text{OH}^-]}{[\text{H}_2\text{O}]} \quad (\text{C.7})$$

$$K_4 = \frac{[H^+][CO_3^{2-}]}{[HCO_3^-]} \quad (C.8)$$

The overall material and charge balance equations are written as:

$$[\text{Amine}] = [\text{RNH}_2] + [\text{RNH}_3^+] \quad (C.9)$$

$$[\text{Amine}]\alpha = [\text{CO}_2] + [\text{HCO}_3^-] + [\text{CO}_3^{2-}] \quad (C.10)$$

$$[\text{RNH}_3^+] + [\text{H}^+] = [\text{OH}^-] + [\text{HCO}_3^-] + 2[\text{CO}_3^{2-}] \quad (C.11)$$

where α is loading capacity, which means the total number of moles of CO_2 absorbed in one mole of Amine

The physical solubility of CO_2 in absorbents is related to the partial pressure of CO_2 by Henry's law as:

$$P_{\text{CO}_2} = H_{\text{CO}_2} [\text{CO}_2] \quad (C.12)$$

By solving Eqs. (C.5)-(C.11), the concentrations of seven species (i.e., $[\text{RNH}_2]$, $[\text{H}^+]$, $[\text{RNH}_3^+]$, $[\text{HCO}_3^-]$, $[\text{CO}_2]$, $[\text{OH}^-]$, $[\text{CO}_3^{2-}]$) and K_1 are found for the given values of $[\text{Amine}]$, α , P_{CO_2} , H_{CO_2} , K_2 , K_3 and K_4 . The equilibrium constants of Eqs. (C.2)-(C.4) and Henry's law constant are calculated from the correlations given in Kent and Eisenberg (1976) as:

$$K_2 = \exp(-241.818 + 298.253 \times 10^3/T - 148.528 \times 10^6/T^2 + 332.648 \times 10^3/T^3 - 282.394 \times 10^{10}/T^4) \quad (C.13)$$

$$K_3 = \exp(3.5554 - 987.9 \times 10^2/T + 568.828 \times 10^5/T^2 - 146.451 \times 10^8/T^3 + 136.146 \times 10^{10}/T^4) \quad (C.14)$$

$$K_4 = \exp(-294.74 + 364.385 \times 10^3/T - 184.158 \times 10^6/T^2 + 415.793 \times 10^8/T^3 - 354.291 \times 10^{10}/T^4) \quad (C.15)$$

$$H_{\text{CO}_2} = \exp(22.2819 - 138.306 \times 10^2/T + 691.346 \times 10^4/T^2 - 155.895 \times 10^7/T^3 + 120.037 \times 10^9/T^4) / 7.50061 \quad (C.16)$$

The apparent equilibrium constant, K_1 , of Eq. (C.5) representing the amine reaction is assumed to be a function of temperature, amine concentration and CO_2 loading following the method of Li and Shen (1993).

$$K_1 = \exp(a_1 + a_2/T + a_3/T^3 + b_1\alpha + b_2/\alpha T + b_3/\alpha^2 + b_4 \ln m) \quad (\text{C.17})$$

where m is Amine concentration in molarity.

The constants, a_1 and b_1 , in Eq. (C.17) are determined by a least-squares fit to the experimental solubility data. Using these parameters, the solubility of CO_2 in aqueous amine solutions can be calculated by solving the above nonlinear equations by Muller's method.



ศูนย์วิทยทรัพยากร
จุฬาลงกรณ์มหาวิทยาลัย

VITA

Miss Kidakarn Sangduan was born in Ubonratchatani on June 13, 1984. She received the Bachelor degree of Science in Chemical Technology from Department of Chemical Technology, Chulalongkorn University in 2006.



ศูนย์วิทยทรัพยากร
จุฬาลงกรณ์มหาวิทยาลัย